Олигоцен-квартер Восточно-Европейской платформы

СТРАТИГРАФИЧЕСКАЯ (ГЕОХРОНОЛОГИЧЕСКАЯ) ШКАЛА. Кайнозой и мезозой

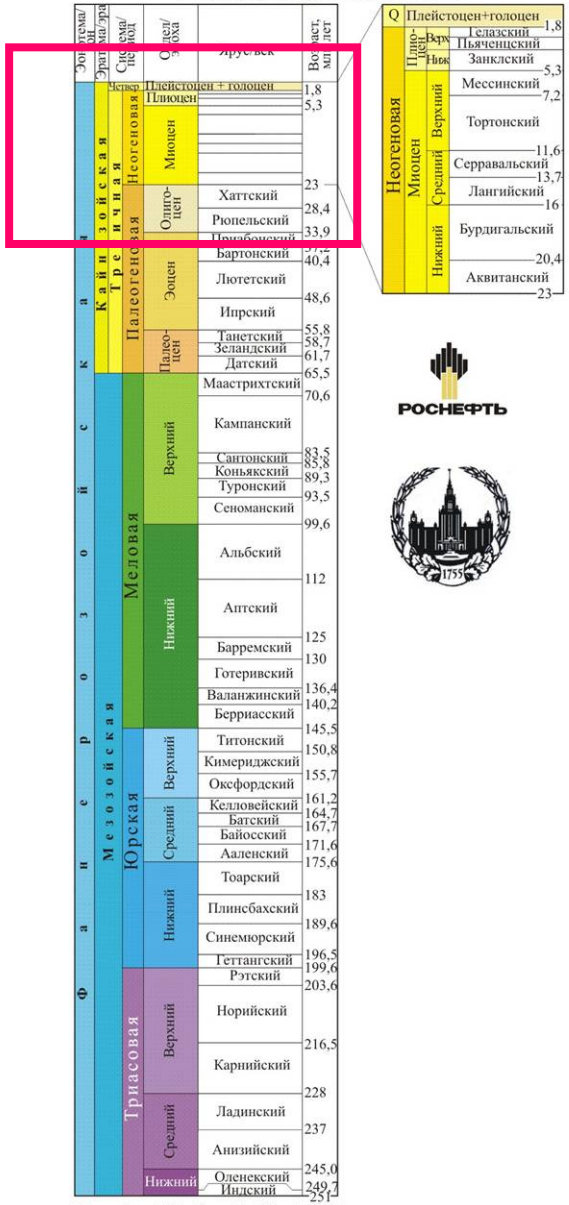

International Stratigraphic Chart, 2004
* Стратиграфический кодекс России, ВСЕГЕИ, 2006

Геологический факультет
МГУ им. М.В. Ломоносова
Корпоративный научно-технический центр "НК "Роснефть"

Составили: Никишин А.М., Алексеев А.С.,
Алисова Е.А., Данилевская Н.С.
декабрь, 2007 г.

РОСНЕФТЬ

1755

СТРАТИГРАФИЧЕСКАЯ (ГЕОХРОНОЛОГИЧЕСКАЯ) ШКАЛА. Палеозой

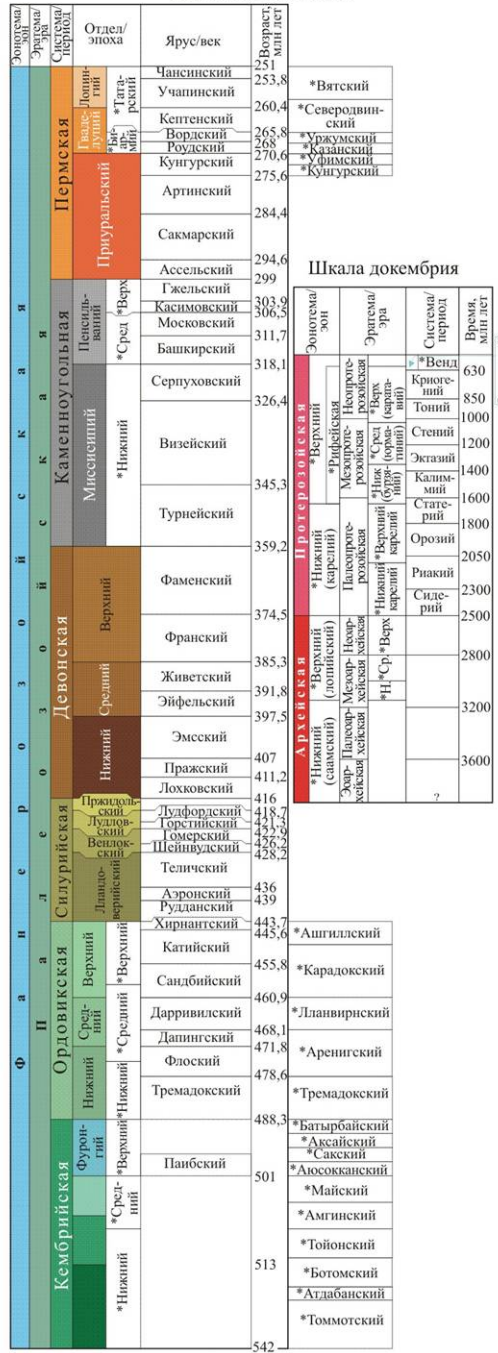

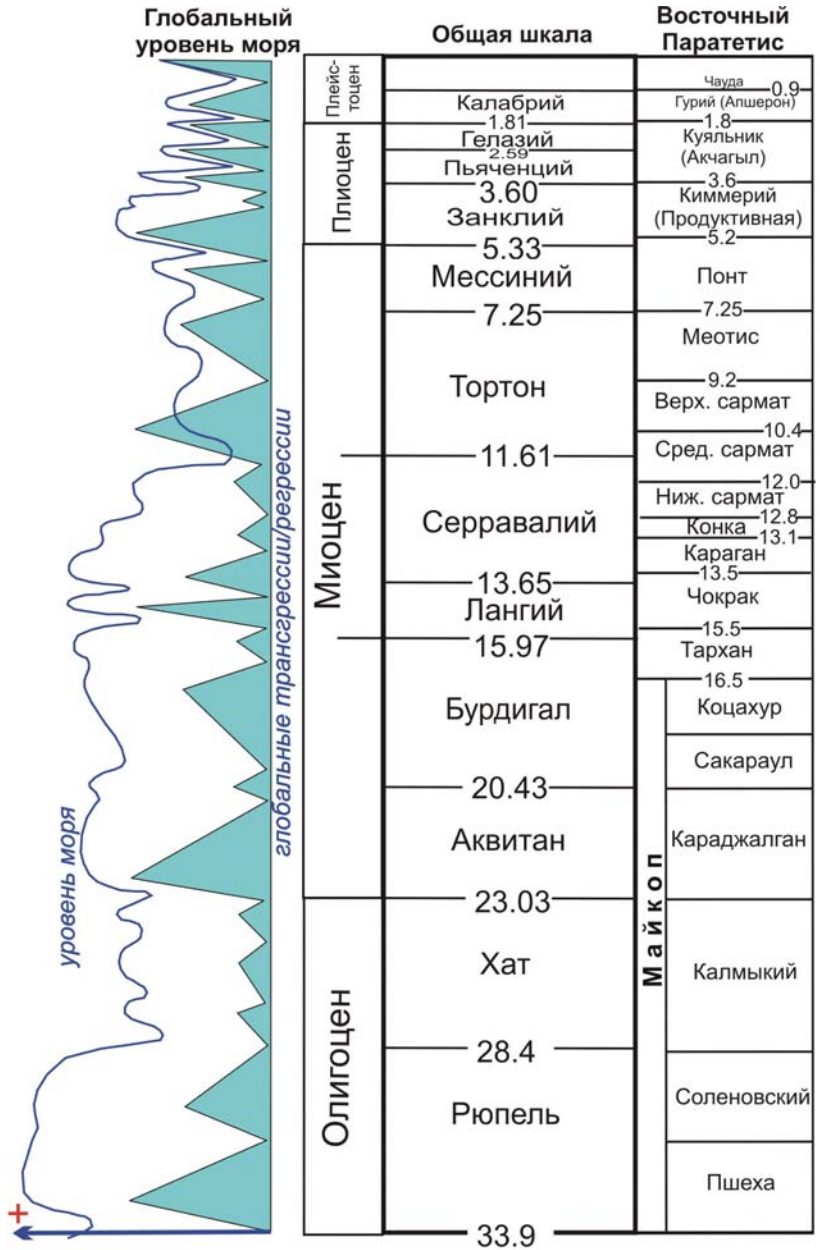
Глобальный уровень моря
Общая шкала
Восточный Паратетис
уровень моря
глобальные трансгрессии/регрессии
+
Плейс-тоцен
Плиоцен
Миоцен
Олигоцен
Калабрий
1.81
Гелазий
2.59
Пьяченций
3.60
Занклий
5.33
Мессиний
7.25
Тортон
11.61
Серравалий
13.65
Лангий
15.97
Бурдигал
20.43
Аквитан
23.03
Хат
28.4
Рюпель
33.9
Чауда
0.9
Гурий (Апшерон)
1.8
Куяльник (Акчагыл)
3.6
Киммерий (Продуктивная)
5.2
Понт
7.25
Меотис
9.2
Верх. сармат
10.4
Сред. сармат
12.0
Ниж. сармат
12.8
Конка
13.1
Караган
13.5
Чокрак
15.5
Тархан
16.5
Майкоп
Коцахур
Сакараул
Караджалган
Калмыкий
Соленовский
Пшеха

Эвстатическая кривая для фанерозоя

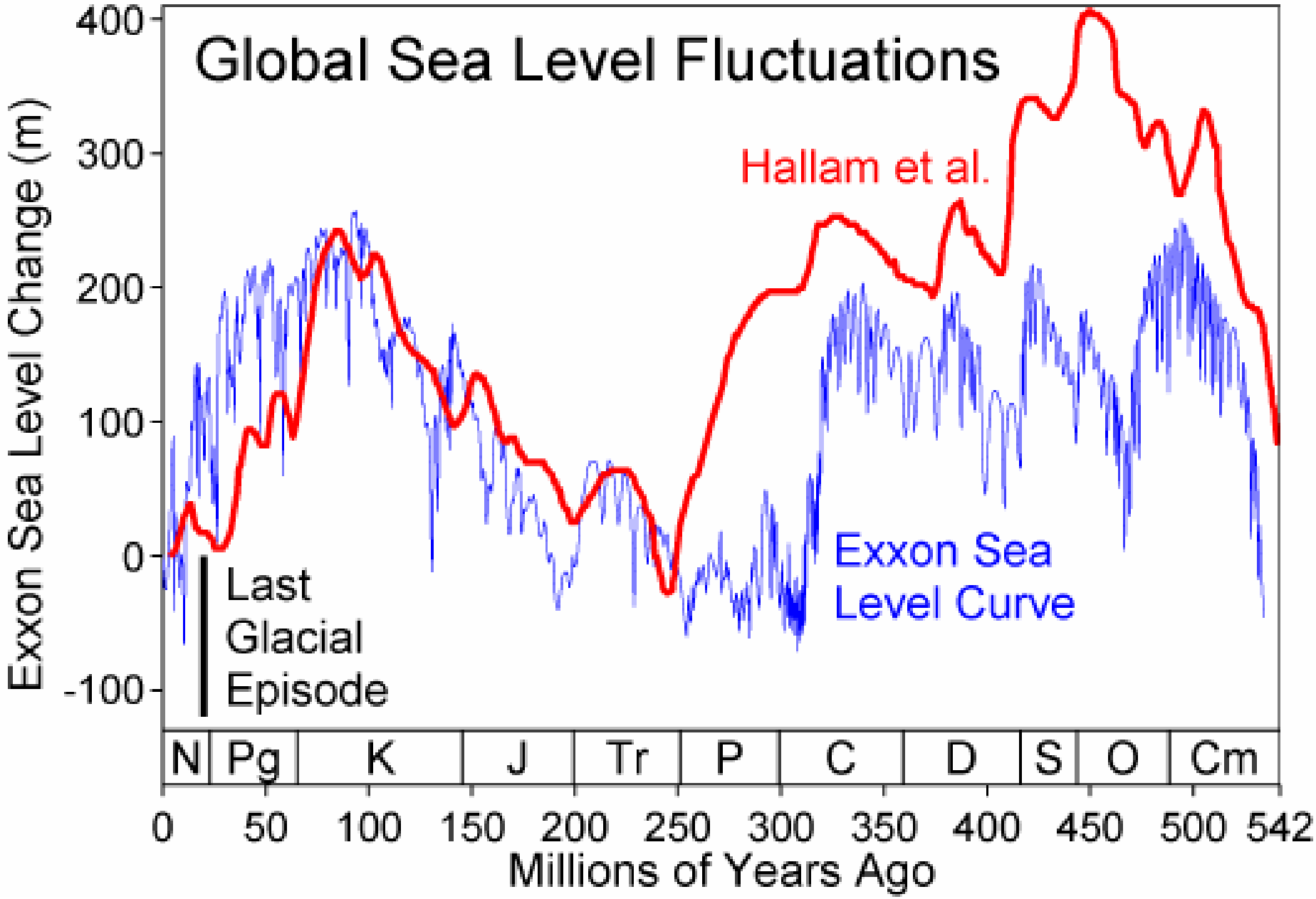

PALEOMAP – Early Oligocene

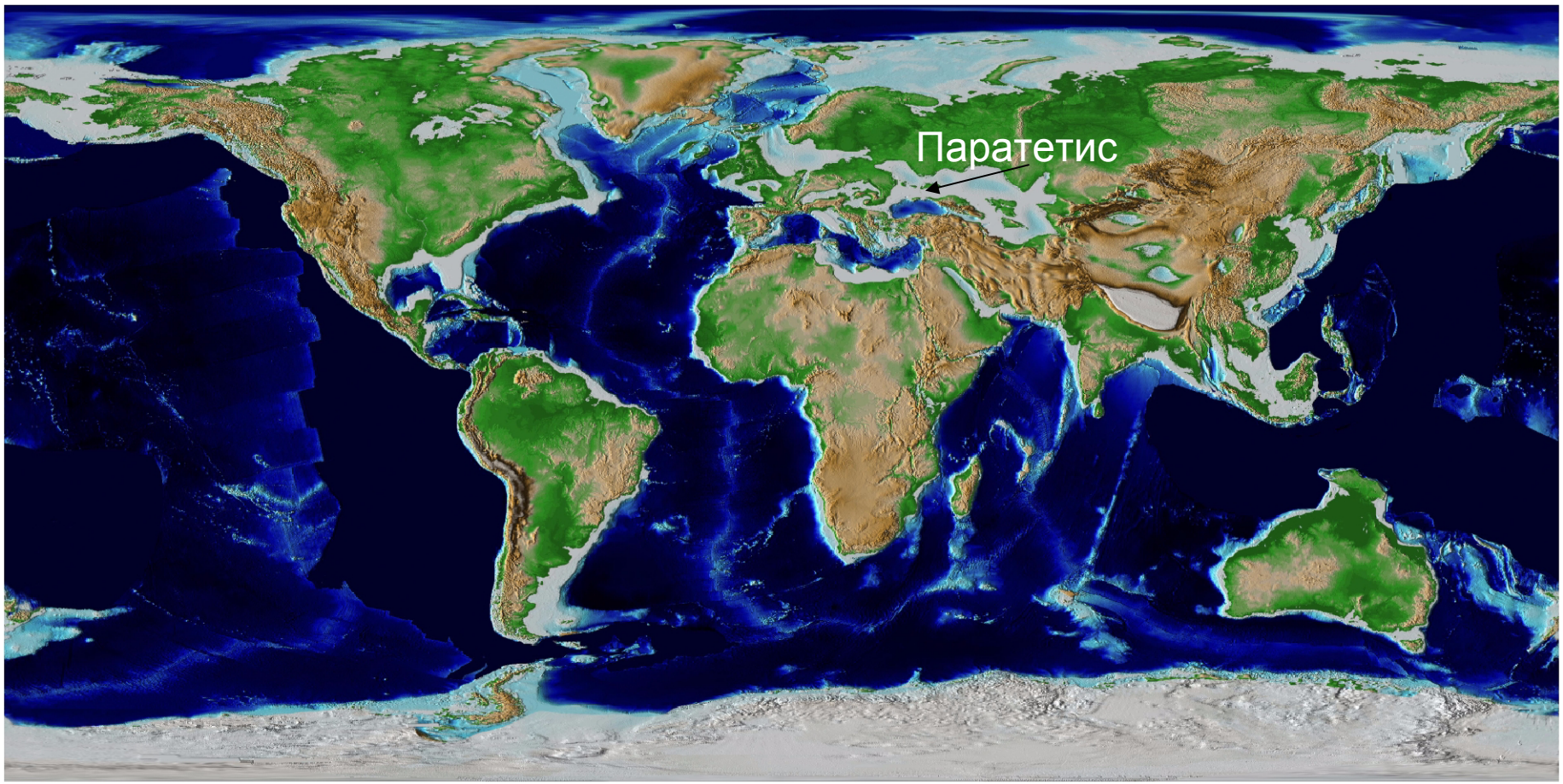

Поздний эоцен, приабон, белоглинка

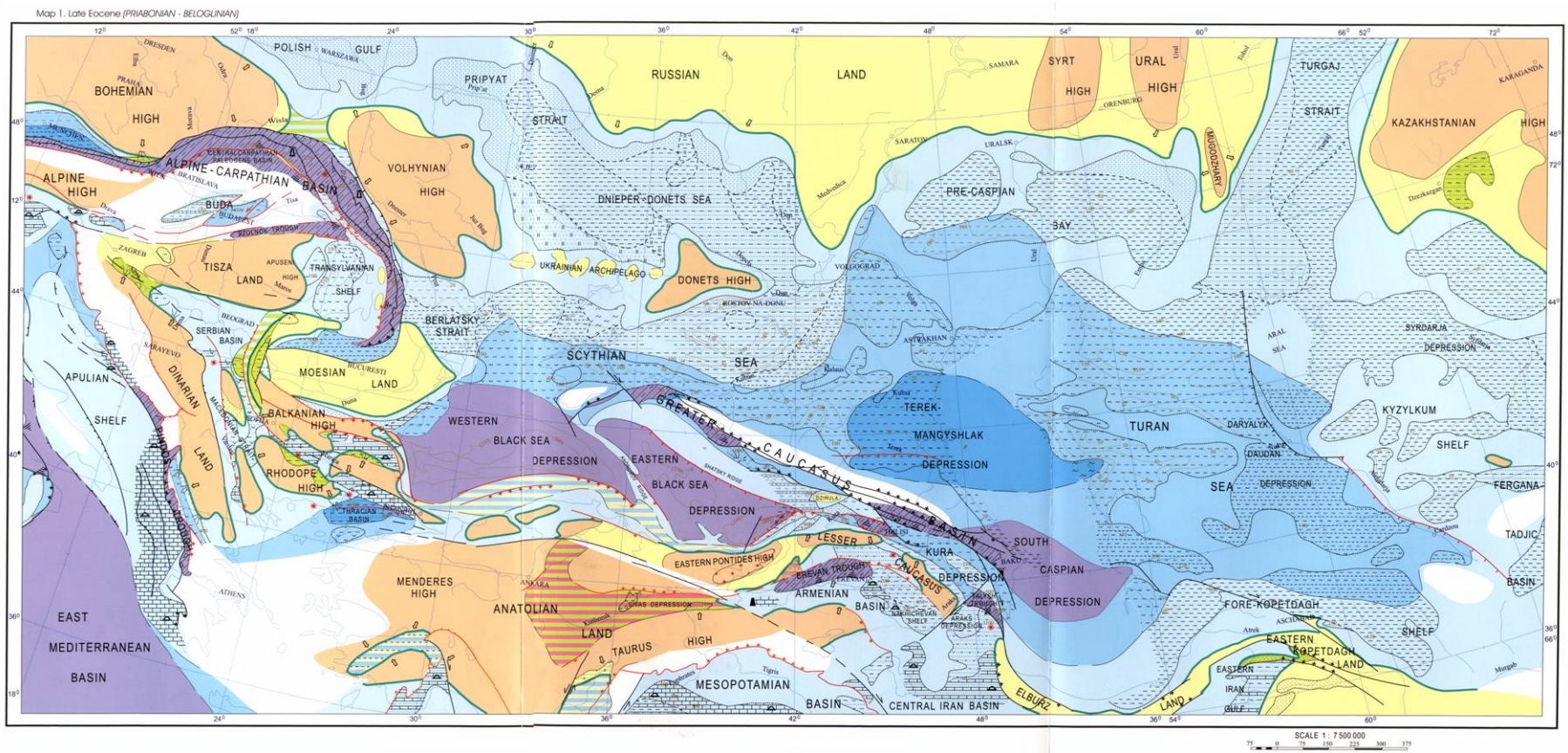

Попов и др, 2004

Ранний олигоцен,ранний рюпель, пшеха

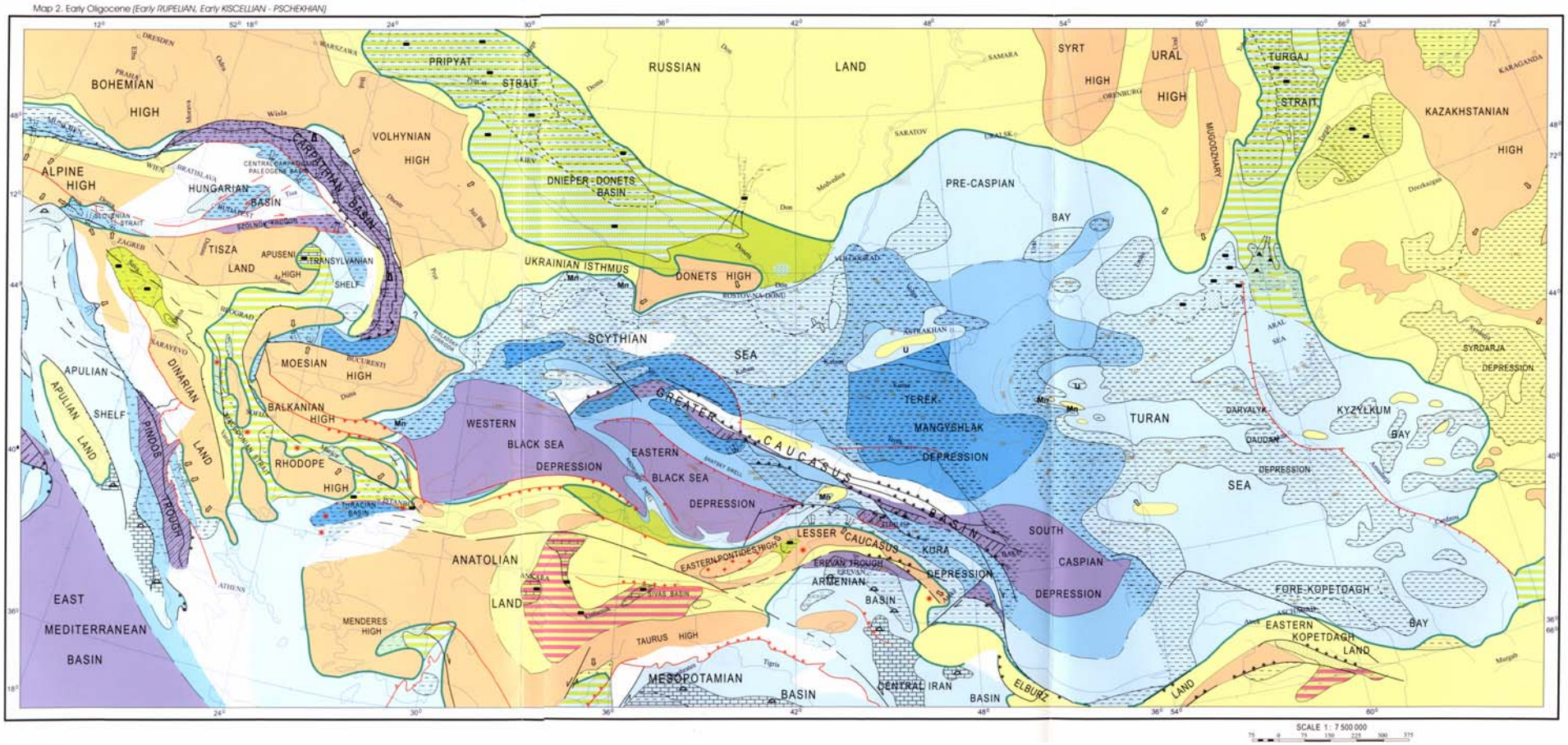

Попов и др, 2004

Поздний олигоцен, хат, калмыкий

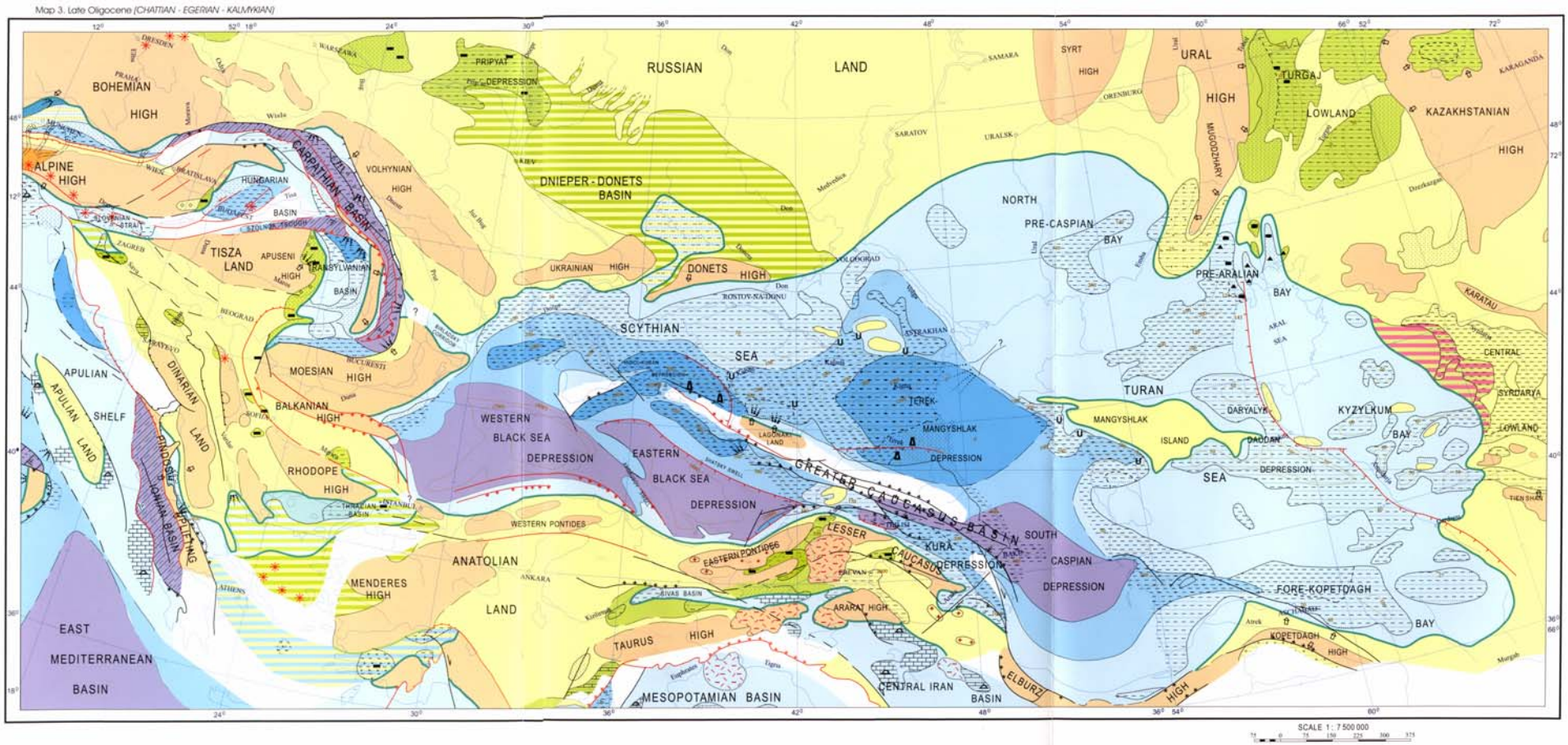

Попов и др, 2004

Ранний миоцен, бурдигал, сакараул

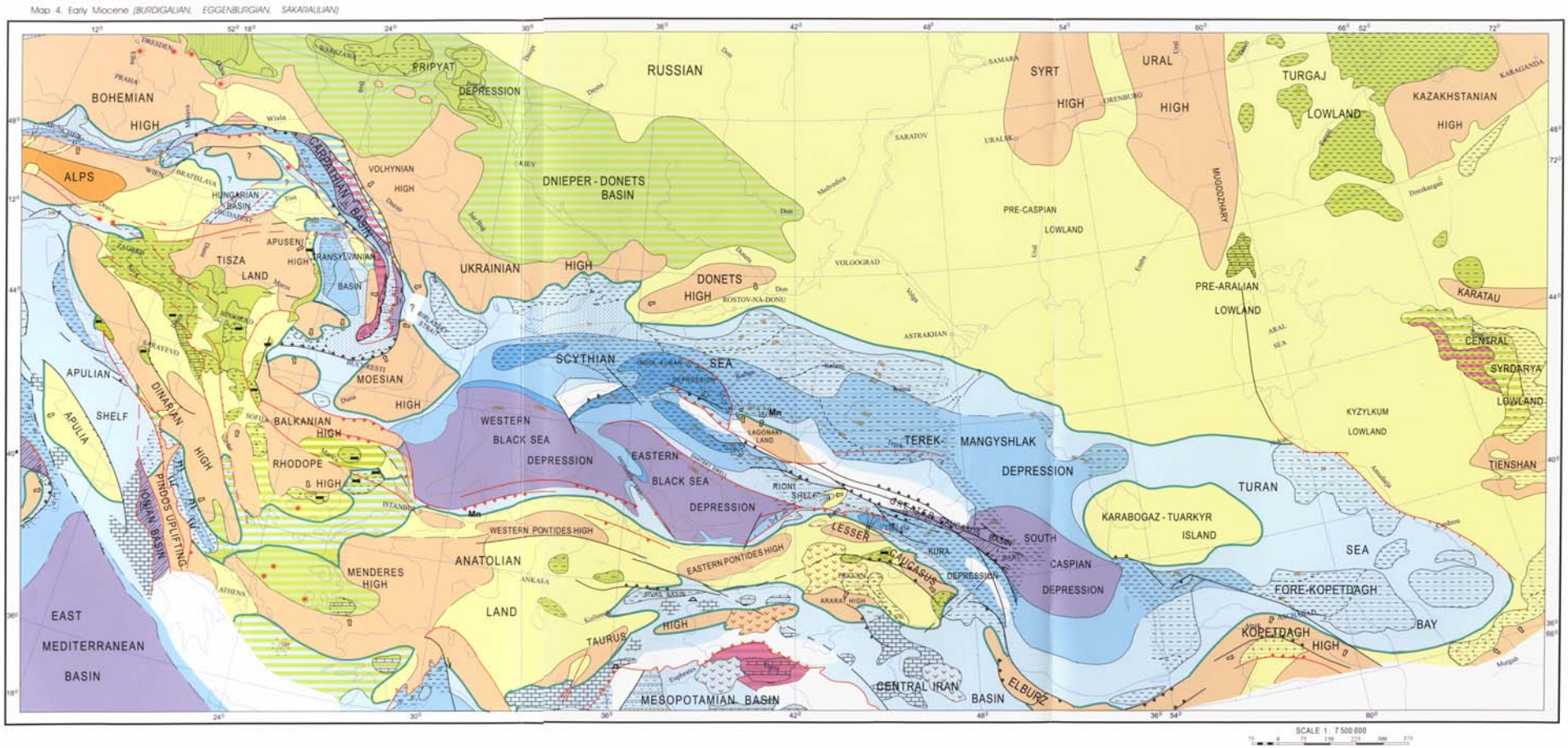

Попов и др, 2004

Средний миоцен, лангий, чокрак

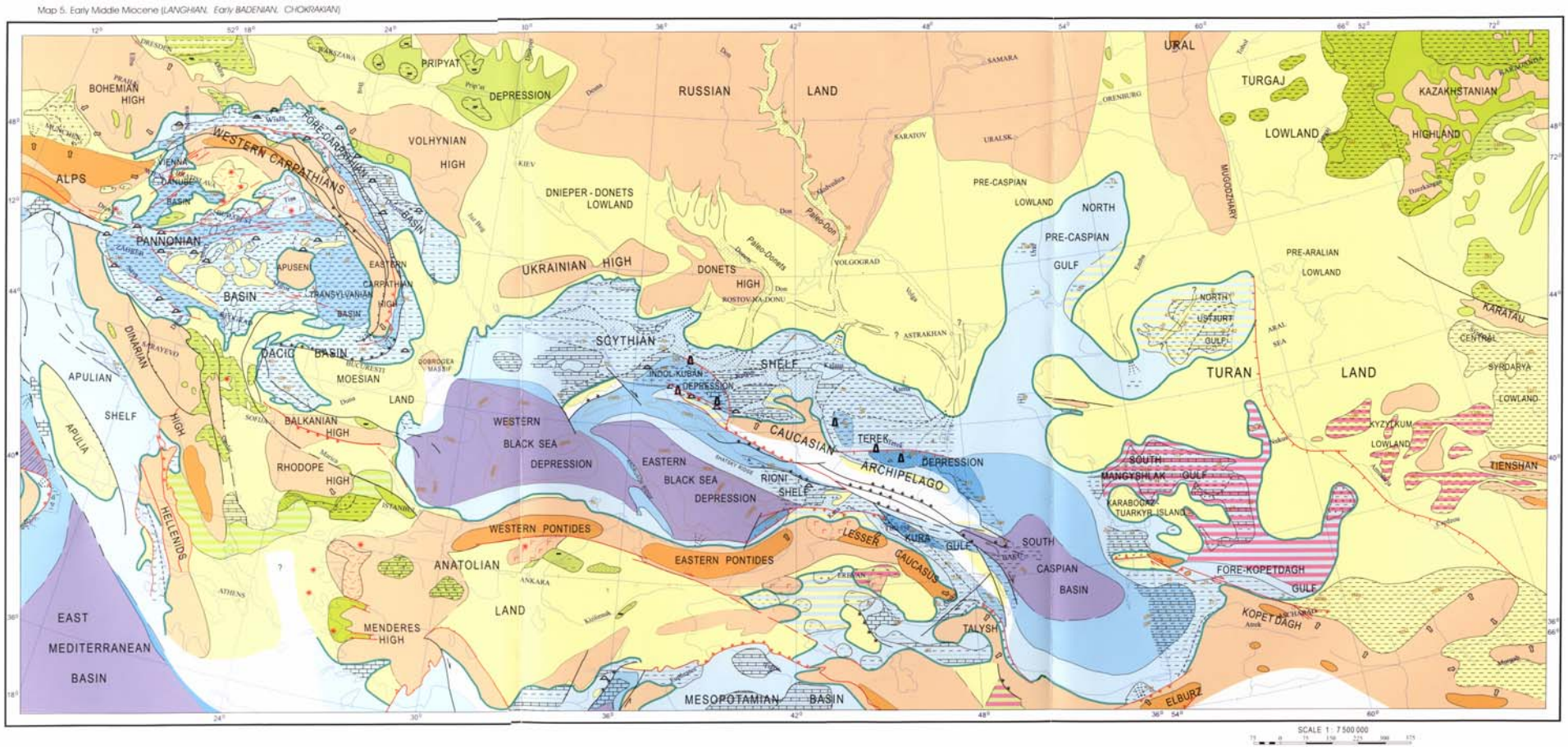

Попов и др, 2004

Средний миоцен, средний серравалий, конка

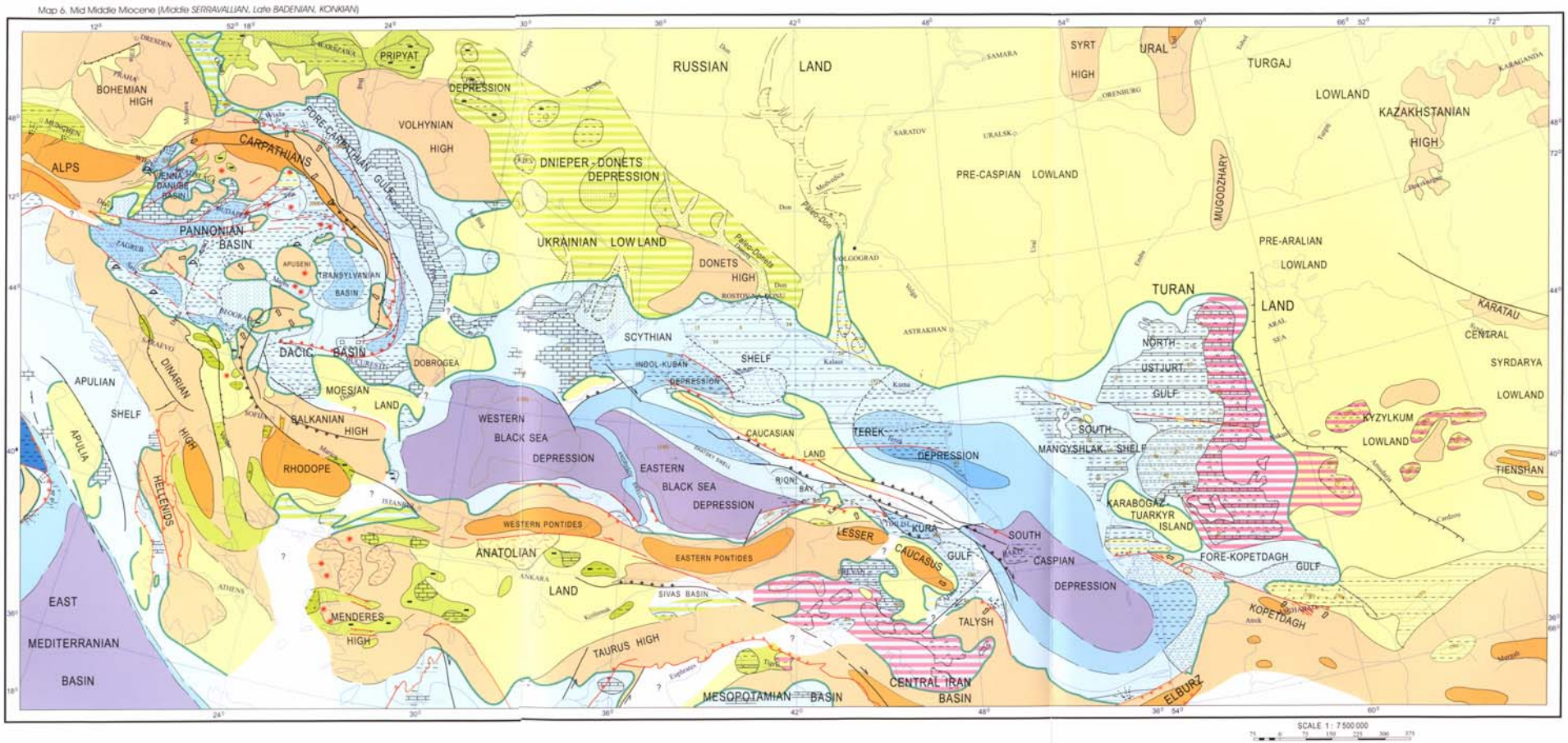

Попов и др, 2004

Средний-поздний миоцен, конец серравалия – начало тортона, средний сармат

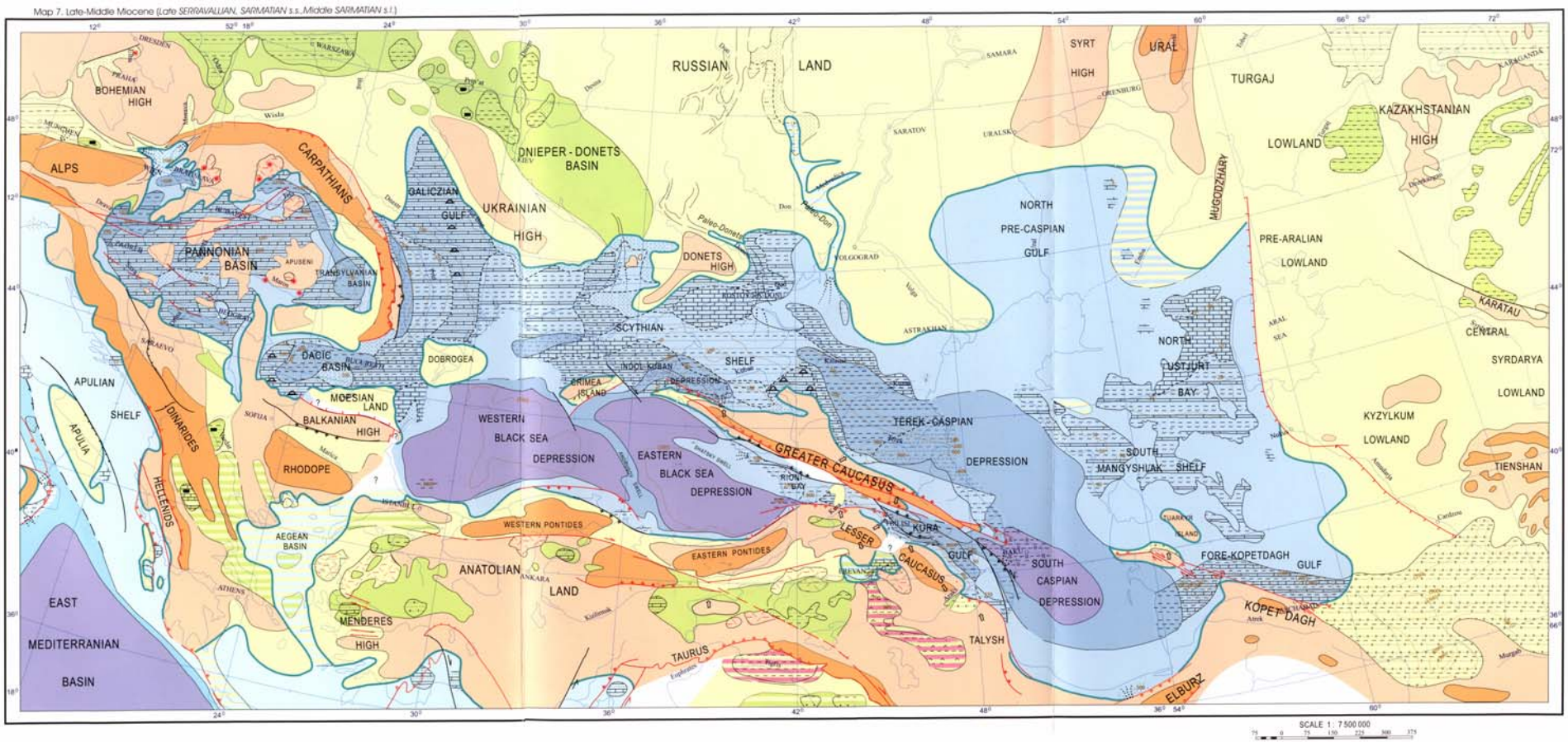

Попов и др, 2004

Поздний миоцен, поздний тортон, ранний меотис

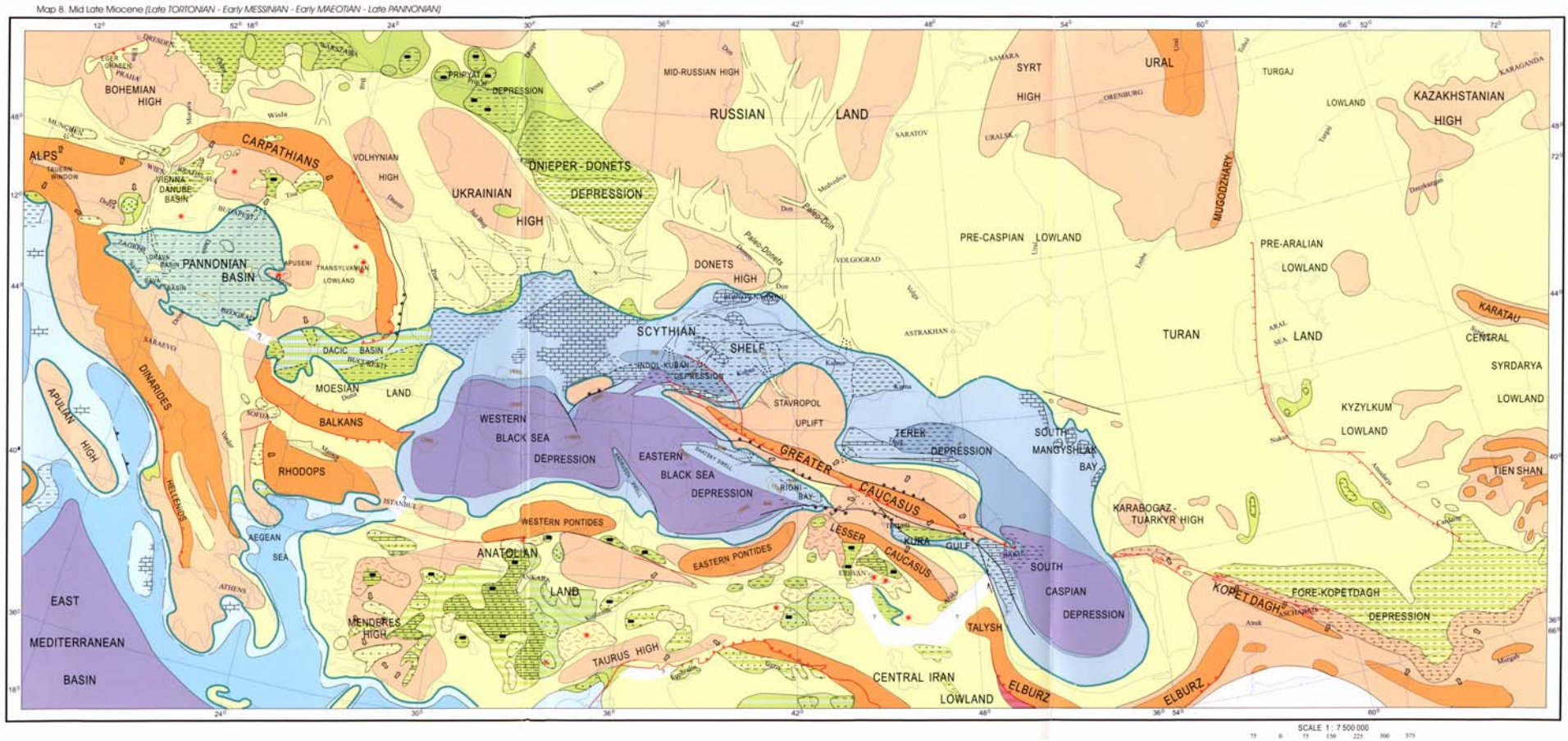

Попов и др, 2004

Поздний миоцен, мессиний, ранний понт

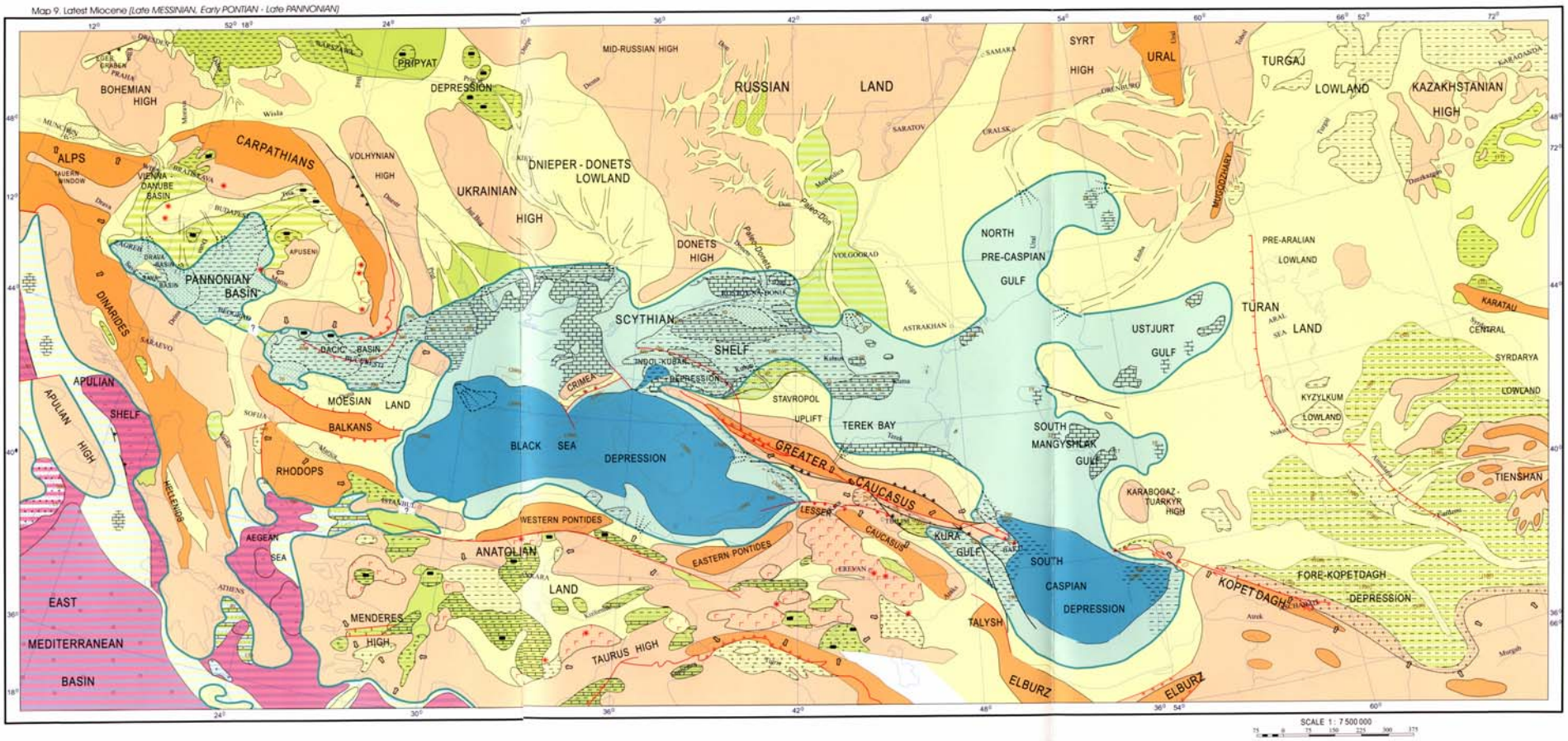

Попов и др, 2004

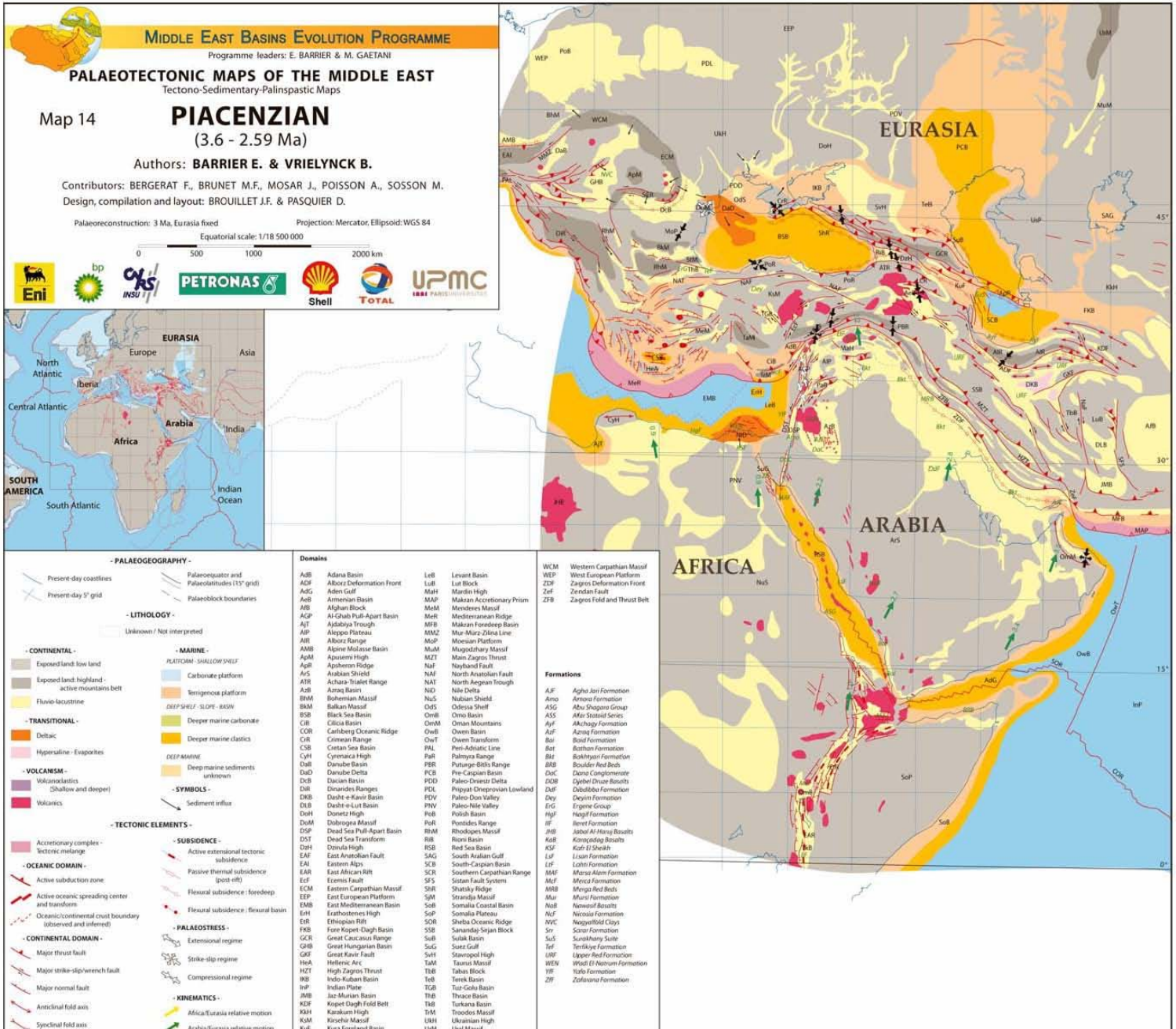
MIDDLE EAST BASINS EVOLUTION PROGRAMME
Programme leaders: E. BARRIER & M. GAETANI
PALAEOTECTONIC MAPS OF THE MIDDLE EAST
Tectono-Sedimentary-Palinspastic Maps
Map 14
PIACENZIAN
(3.6 - 2.59 Ma)
Authors: BARRIER E. & VRIELYNCK B.
Contributors: BERGERAT F., BRUNET M.F., MOSAR J., POISSON A., SOSSON M.
Design, compilation and layout: BROUILLET J.F. & PASQUIER D.
Palaeoreconstruction: 3 Ma, Eurasia fixed
Projection: Mercator, Ellipsoid: WGS 84
Equatorial scale: 1/18 500 000
0 500 1000 2000 km
Eni
bp
INSU
PETRONAS
Shell
TOTAL
UPMC
EURASIA
ARABIA
AFRICA
North Atlantic
Europe
Asia
Iberia
Central Atlantic
Arabia
India
Africa
SOUTH AMERICA
South Atlantic
Indian Ocean
- PALAEOGEOGRAPHY -
Present-day coastlines
Present-day 5° grid
Palaeoequator and Palaeolatitudes (15° grid)
Palaeoblock boundaries
- LITHOLOGY -
Unknown / Not interpreted
- CONTINENTAL -
Exposed land: low land
Exposed land: highland - active mountains belt
Fluvio-lacustrine
- TRANSITIONAL -
Deltaic
Hypersaline - Evaporites
- VOLCANISM -
Volcanoclastics (Shallow and deeper)
Volcanics
- MARINE -
PLATFORM - SHALLOW SHELF
Carbonate platform
Terrigenous platform
DEEP SHELF - SLOPE - BASIN
Deeper marine carbonate
Deeper marine clastics
DEEP MARINE
Deep marine sediments unknown
- SYMBOLS -
Sediment influx
- TECTONIC ELEMENTS -
Accretionary complex - Tectonic melange
- OCEANIC DOMAIN -
Active subduction zone
Active oceanic spreading center and transform
Oceanic/continental crust boundary (observed and inferred)
- CONTINENTAL DOMAIN -
Major thrust fault
Major strike-slip/wrench fault
Major normal fault
Anticlinal fold axis
Synclinal fold axis
- SUBSIDENCE -
Active extensional tectonic subsidence
Passive thermal subsidence (post-rift)
Flexural subsidence : foredeep
Flexural subsidence : flexural basin
- PALAEOSTRESS -
Extensional regime
Strike-slip regime
Compressional regime
- KINEMATICS -
Africa/Eurasia relative motion
Arabia/Eurasia relative motion
Domains
AdB Adana Basin
ADF Alborz Deformation Front
AdG Aden Gulf
AeB Armenian Basin
AfB Afghan Block
AGP Al Ghab Pull-Apart Basin
AjT Ajdabiya Trough
AlP Aleppo Plateau
AlR Alborz Range
AMB Alpine Molasse Basin
ApM Apuseni High
ApR Apsheron Ridge
ArS Arabian Shield
ATR Achara-Trialet Range
AzB Azraq Basin
BhM Bohemian Massif
BkM Balkan Massif
BSB Black Sea Basin
CiB Cilicia Basin
COR Carlsberg Oceanic Ridge
CrR Crimean Range
CSB Cretan Sea Basin
CyH Cyrenaica High
DaB Danube Basin
DaD Danube Delta
DcB Dacian Basin
DiR Dinarides Ranges
DKB Dasht-e-Kavir Basin
DLB Dasht-e-Lut Basin
DoH Donetz High
DoM Dobrogea Massif
DSP Dead Sea Pull-Apart Basin
DST Dead Sea Transform
DzH Dzinula High
EAF East Anatolian Fault
EAl Eastern Alps
EAR East African Rift
EcF Ecemis Fault
ECM Eastern Carpathian Massif
EEP East European Platform
EMB East Mediterranean Basin
ErH Erathostenes High
EtR Ethiopian Rift
FKB Fore Kopet-Dagh Basin
GCR Great Caucasus Range
GHB Great Hungarian Basin
GKF Great Kavir Fault
HeA Hellenic Arc
HZT High Zagros Thrust
IKB Indo-Kuban Basin
InP Indian Plate
JMB Jaz-Murian Basin
KDF Kopet Dagh Fold Belt
KkH Karakum High
KsM Kirsehir Massif
LeB Levant Basin
LuB Lut Block
MaH Mardin High
MAP Makran Accretionary Prism
MeM Menderes Massif
MeR Mediterranean Ridge
MFB Makran Foredeep Basin
MMZ Mur-Mürz-Zilina Line
MoP Moesian Platform
MuM Mugodzhary Massif
MZT Main Zagros Thrust
NaF Nayband Fault
NAF North Anatolian Fault
NAT North Aegean Trough
NiD Nile Delta
NuS Nubian Shield
OdS Odessa Shelf
OmB Omo Basin
OmM Oman Mountains
OwB Owen Basin
OwT Owen Transform
PAL Peri-Adriatic Line
PaR Palmyra Range
PBR Puturge-Bitlis Range
PCB Pre-Caspian Basin
PDD Paleo-Dniestr Delta
PDL Pripyat-Dneprovian Lowland
PDV Paleo-Don Valley
PNV Paleo-Nile Valley
PoB Polish Basin
PoR Pontides Range
RhM Rhodopes Massif
RiB Rioni Basin
RSB Red Sea Basin
SAG South Aralian Gulf
SCB South-Caspian Basin
SCR Southern Carpathian Range
SFS Sistan Fault System
ShR Shatsky Ridge
SjM Strandja Massif
SoB Somalia Coastal Basin
SoP Somalia Plateau
SOR Sheba Oceanic Ridge
SSB Sanandaj-Sirjan Block
SuB Sulak Basin
SuG Suez Gulf
SvH Stavropol High
TaM Taurus Massif
TbB Tabas Block
TeB Terek Basin
TGB Tuz-Golu Basin
ThB Thrace Basin
TkB Turkana Basin
TrM Troodos Massif
UkH Ukrainian High
WCM Western Carpathian Massif
WEP West European Platform
ZDF Zagros Deformation Front
ZeF Zendan Fault
ZFB Zagros Fold and Thrust Belt
Formations
AJF Agha Jari Formation
Amo Amora Formation
ASG Abu Shagara Group
ASS Afar Stratoid Series
AyF Akchagy Formation
AzF Azraq Formation
Bai Baid Formation
Bat Bathian Formation
Bkt Bakhtyari Formation
BRB Boulder Red Beds
DaC Dana Conglomerate
DdB Djebel Druze Basalts
DdF Dabdibba Formation
Dey Deyim Formation
ErG Ergene Group
HgF Hagif Formation
IlF Ileret Formation
JhB Jabal Al-Haruj Basalts
KaB Karacadag Basalts
KSF Kath El Sheikh
LsF Lisan Formation
LtF Lahti Formation
MAF Marsa Alam Formation
MeF Mereja Formation
MRB Mereja Red Beds
Mur Mursi Formation
NaB Nawasif Basalts
NcF Necasia Formation
NVC Neogyalfold Clays
Srr Sarar Formation
SuS Surakhany Suite
TeF Terrikyar Formation
URF Upper Red Formation
WEN Wadi El Natrum Formation
YIF Yafo Formation
ZFF Zafarana Formation

Поздний плиоцен, гелазий, акчагыл

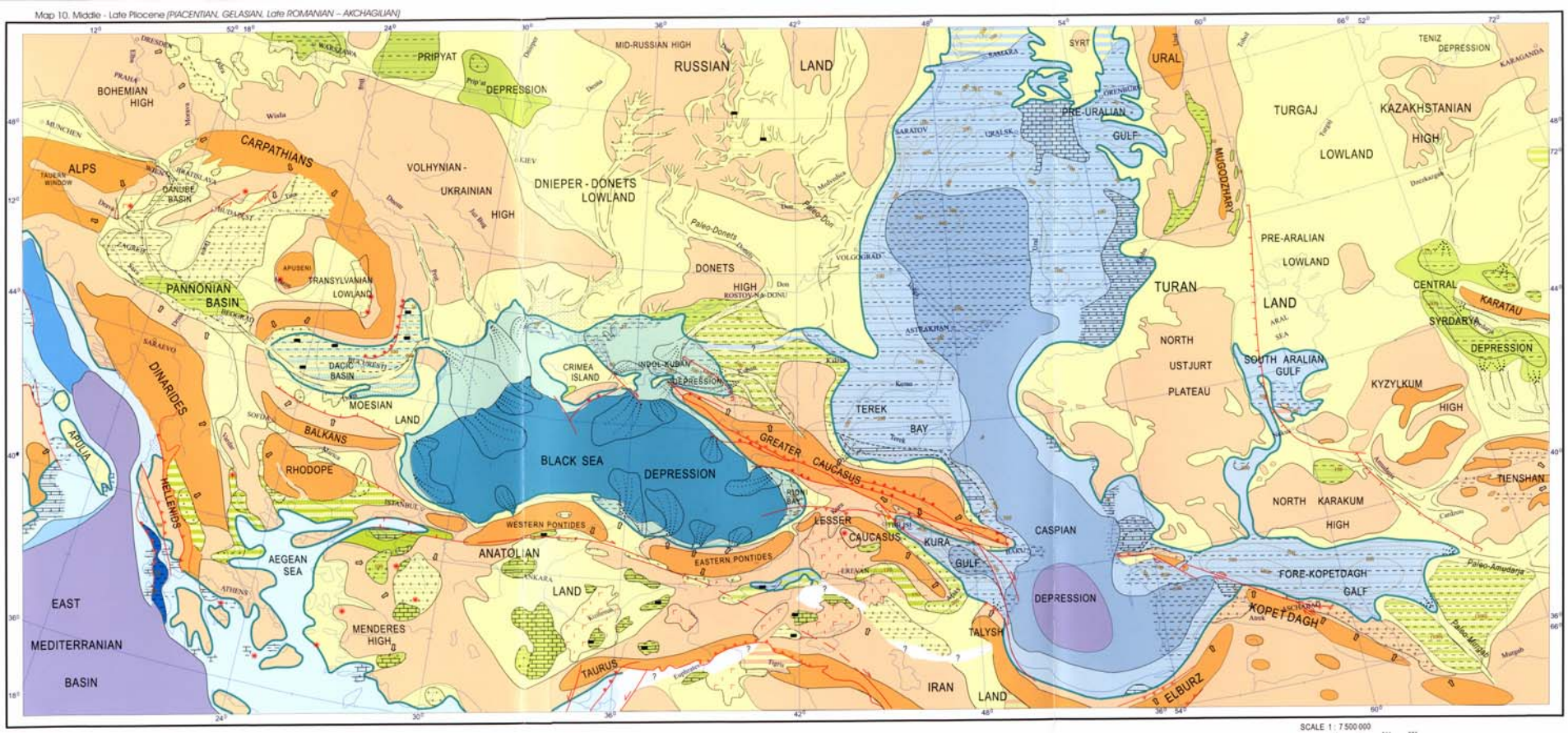

Попов и др, 2004

Схема неотектоники

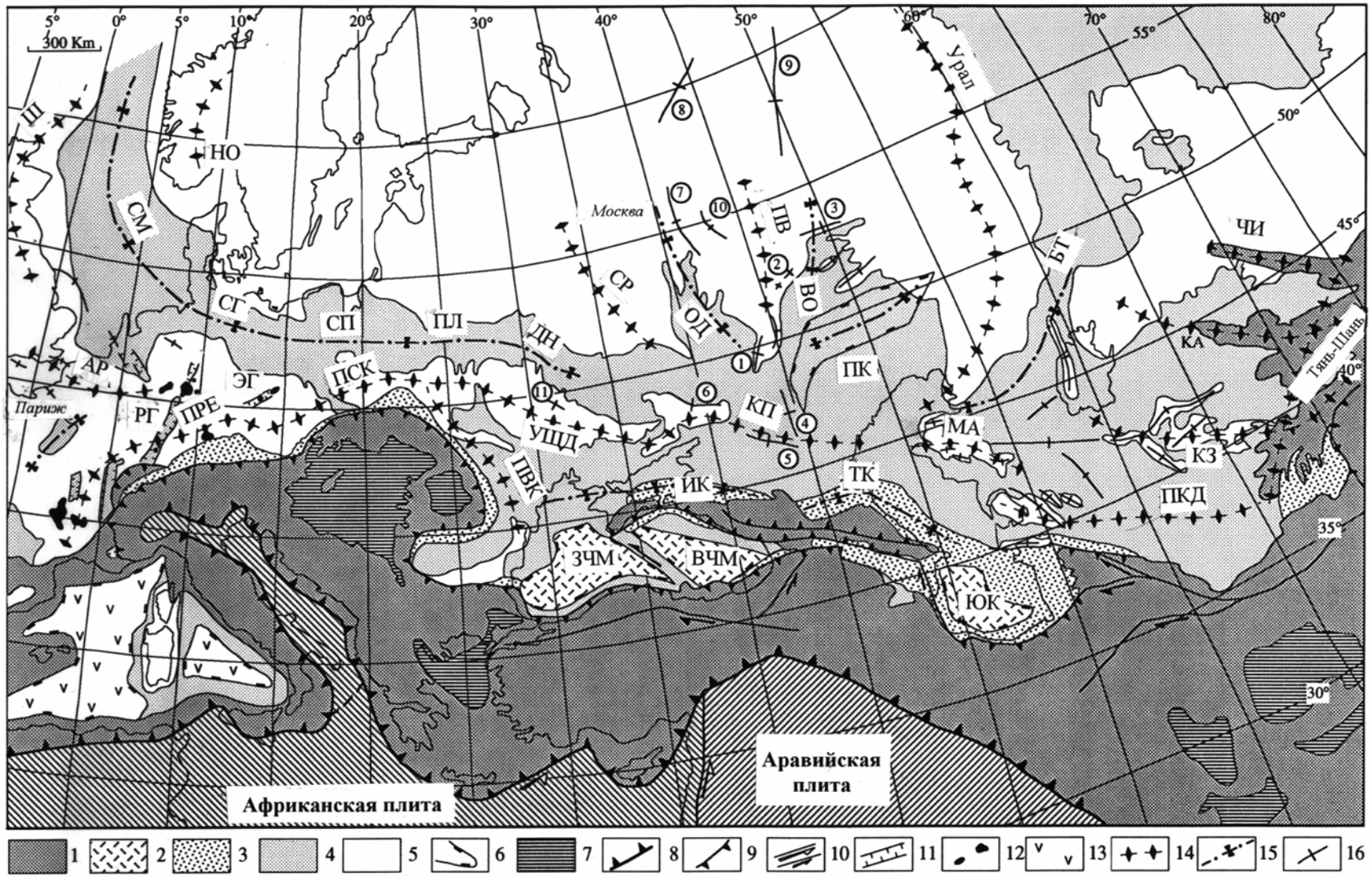

Схема неотектоники

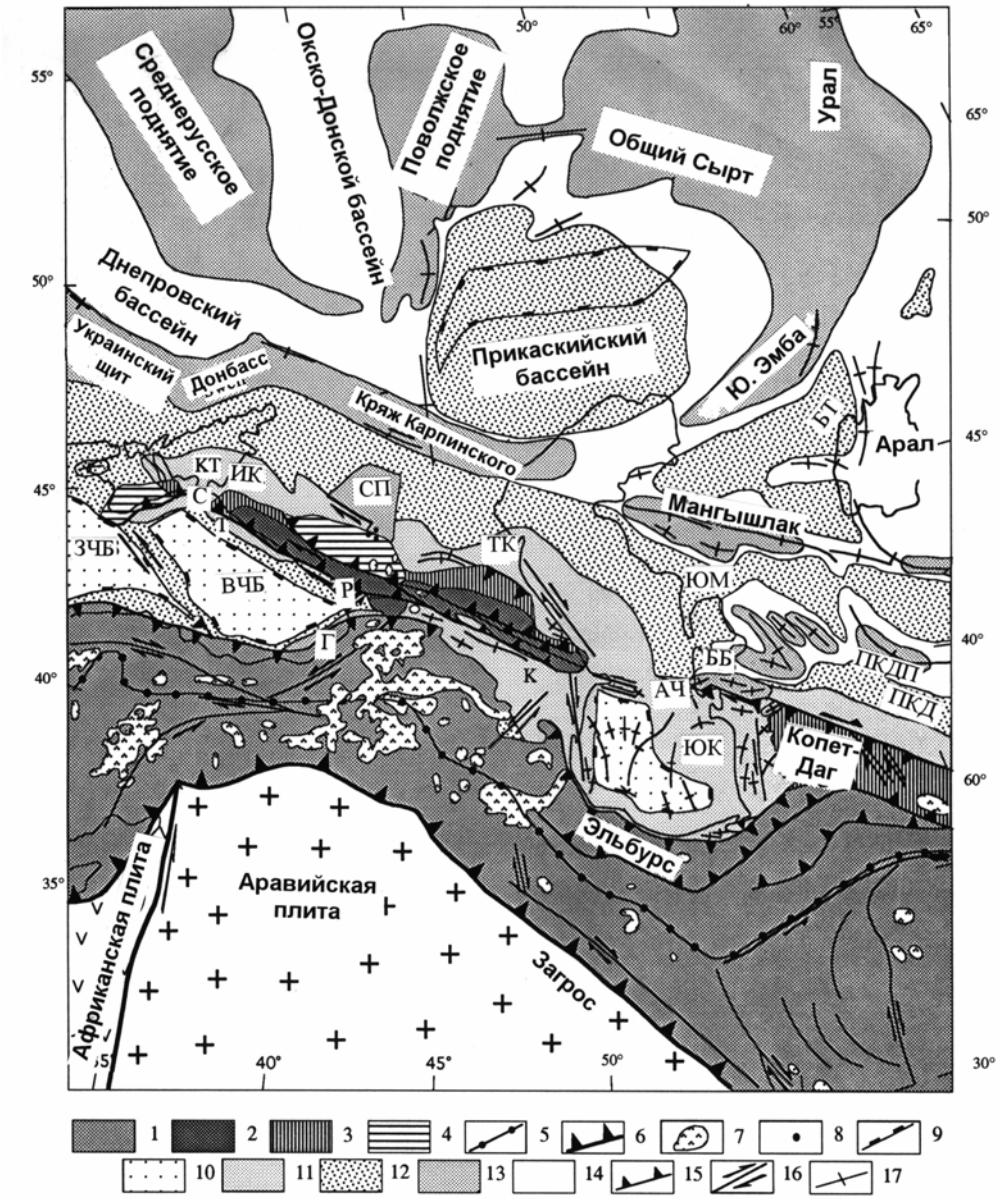

INTERNATIONAL STRATIGRAPHIC CHART

International Commission on Stratigraphy

ICS

IUGS

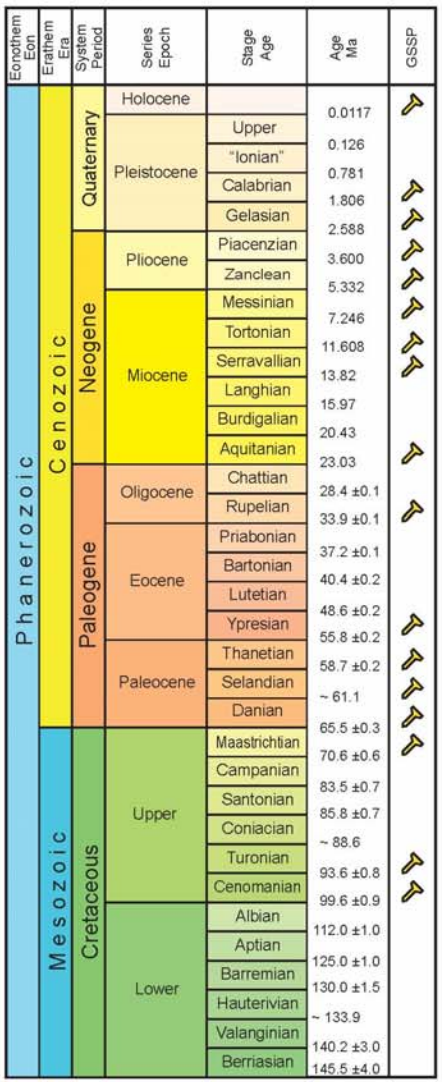

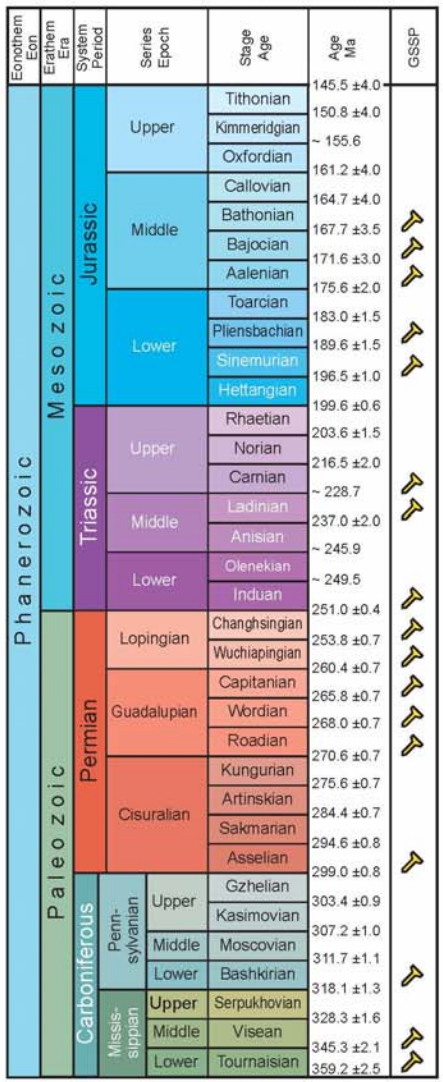

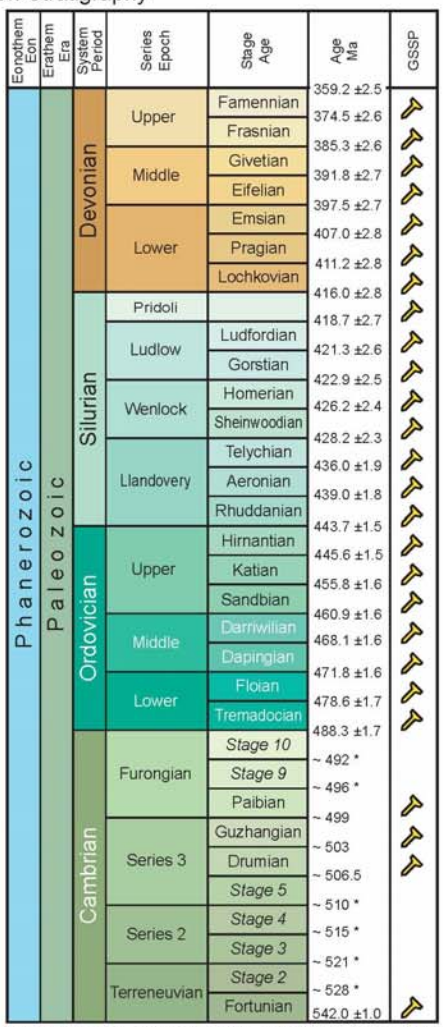

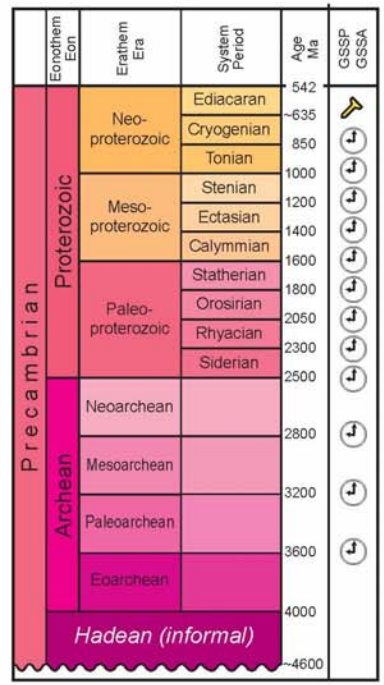

This chart was drafted by Gabi Ogg. Intra Cambrian unit ages with * are informal, and awaiting ratified definitions.

Subdivisions of the global geologic record are formally defined by their lower boundary. Each unit of the Phanerozoic (~542 Ma to Present) and the base of Ediacaran are defined by a basal Global Boundary Stratotype Section and Point (GSSP), whereas Precambrian units are formally subdivided by absolute age (Global Standard Stratigraphic Age, GSSA). Details of each GSSP are posted on the ICS website (www.*stratigraphy.org*).

Numerical ages of the unit boundaries in the Phanerozoic are subject to revision. Some stages within the Cambrian will be formally named upon international agreement on their GSSP limits. Most sub-Series boundaries (e.g., Middle and Upper Aptian) are not formally defined.

Colors are according to the Commission for the Geological Map of the World (www.*cgmw.org*).

The listed numerical ages are from 'A Geologic Time Scale 2004', by F.M. Gradstein, J.G. Ogg, A.G. Smith, et al. (2004; Cambridge University Press) and "The Concise Geologic Time Scale" by J.G. Ogg, G. Ogg and F.M. Gradstein (2008).

August 2009

Global chronostratigraphical correlation table for the last 2.7 million years

v. 2007b

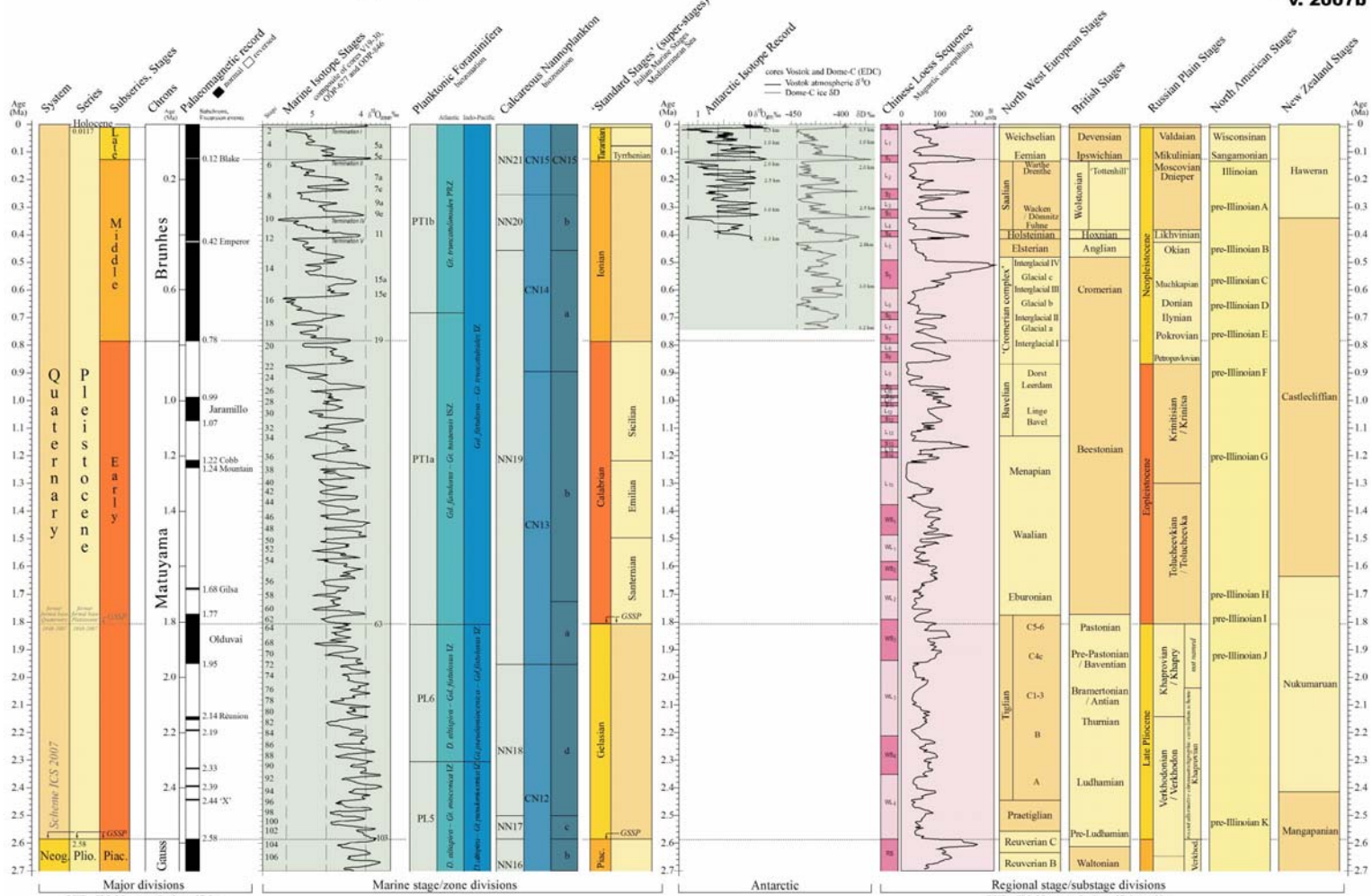

UNIVERSITY OF CAMBRIDGE
http://www.cam.ac.uk/

© Cambridge Quaternary **2007**
Compiled by P.L. Gibbard[1], S. Boreham[1], K.M. Cohen[1] & A. Moscariello[2].
[1]Quaternary Palaeoenvironments Group, Cambridge Quaternary, Department of Geography, University of Cambridge, United Kingdom.
[2]Utrecht Centre of Geosciences, Department of Physical Geography, Faculty of Geosciences, Utrecht University, The Netherlands
http://www-qpg.geog.cam.ac.uk/

International Union of Geological Sciences (IUGS), International Commission on Stratigraphy (ICS), Subcommission on Quaternary Stratigraphy (SQS).
http://www.stratigraphy.org/

INQUA 1928
International Union for Quaternary Research (INQUA), Stratigraphy and Chronology Commission (SACCOM).
http://www.inqua.tcd.ie/

Kindly printed and supported by: **BOREAS**, an international journal of Quaternary research.
Short reference: Gibbard *et al.* 2005, *modified* 2007.
Full reference: Gibbard, P.L., Boreham, S., Cohen, K.M. & Moscariello, A. 2005: Global chronostratigraphical correlation table for the last 2.7 million years. Boreas 34 (1): unpaginated, modified/updated 2007.
http://www.tandf.no/boreas

This table provides a correlation of chronostratigraphical subdivisions of late Cenozoic geological time, spanning the last 2.7 million years. The formal division of the Quaternary is the responsibility of the International Commission on Stratigraphy's (ICS) Subcommission on Quaternary Stratigraphy (SQS), in partnership with the International Union for Quaternary Research's (INQUA) Commission on Stratigraphy and Chronology (SACCOM).

System, Series, Subseries

The timescale is based on the internationally-recognised formal time subdivisions: the Phanerozoic Eon, the Cenozoic Era, the Quaternary System or Period, the Pleistocene and Holocene Series, and finally the Early-Late, Middle, Late Upper Pleistocene Subseries. At present the subseries (Subepoch) divisions of the Pleistocene are not formalised. Series, and thereby systems, are formally-defined based on Global Stratotype Sections and Points (GSSP) of which two have been ratified for the last 2.7 million years. The base of the Quaternary-Pleistocene is defined at 2.58 million years from a GSSP at Monte San Nicola in southern Italy. The chart extends to 2.7 million years, to include the very end of the preceding Piacenzian Stage of the Pliocene Series.

Base of the Quaternary and Pleistocene

Since 1948 there has been a consensus that the boundary should be placed at the first evidence of climatic cooling of ice-age magnitude. This was the original basis for placing the boundary in marine sediments in Calabria, in Italy (Agenius & Pareto, 1965). It is now known that a major cooling occurred earlier, at c.2.55 million years, and even earlier cooling events are known from the Pliocene. Many consider that the basal Quaternary - Pleistocene boundary should logically be removed to this position (Gibbard *et al.* 2005, Bowen & Gibbard, 2007), effectively corresponding to the Gauss - Matuyama magnetic Chron boundary (e.g. Partridge, 1997: Suc *et al.*, 1997). Until ratification by the IUGS in 2007 it, this was the base of the Pliocene Gelasian Stage (Rio *et al.*, 1998), which was already a ratified GSSP (Aguirre & Pasini, 1985).

At the time of publication, there is a growing controversy about the status of the term Tertiary. Like Quaternary, it is generally regarded as a full System/Period but discussions are in progress on whether to adopt the Neogene and Paleogene as full systems/periods, or as subsystems (subperiods) of the Tertiary.

GSSPs

Formal GSSPs for the Pleistocene subseries will be proposed in the near future. The INQUA Commission on Stratigraphy/ICS Working Group on Major Subdivision of the Pleistocene agreed to place the Early-Late / Middle boundary at the Brunhes / Matuyama magnetic reversal Chron boundary (Richmond, 1996), a stratotype locality has yet to be identified. Following recent (re-)evaluation, the Middle - Late Upper boundary is placed, following historical precedent in NW Europe, at the Saalian - Eemian Stage boundary. The former is positioned at the basal-boundary stratotype of the Eemian in the Amsterdam-Terminal borehole, the Netherlands (Gibbard, 2005).

The Holocene is generally regarded as having begun 10,000 radiocarbon years, or 11,650 calibrated (i.e. calendar) years, before present (i.e. before 1950 AD, 'BP') or 11 ¾ decimal lunisolares b2k (before 2000 AD). This boundary will be defined as a Global Standard Stratigraphic Age (GSSA). A stratotype is likely to be defined in an ice core of the Greenland Ice-Core Project (N-GRIP core, at 1492.45m depth, Rasmussen *et al.* 2005†) or the Greenland Ice-Sheet Project (GISP2 core). Or alternatively it may be defined in an annually-laminated lake sequence in western Germany (Litt *et al.*, 2001).

'Standard stages' (super-stages) global division

The desire to divide Quaternary/Pleistocene time into 'standard stages', that is units of approximately the same duration as those in the pre-Quaternary Tertiary time, has been advocated from time to time. The only sequence that has been divided in this way is the shallow marine sequences in the Mediterranean region, especially in southern Italy. For various reasons the scheme was considered unsatisfactory for use beyond this region, correlation being based principally on faunal and pollen biostratigraphy. Renewed investigation in recent years has led to the proposal of units based on multidisciplinary investigation. The Tarantian shallow marine stages are derived from Van Couvering (1997) modified by Cita *et al.* (2006). In view of their duration, covering several climate cycles and periods for which regional stage units of markedly shorter duration have been defined, these 'standard stages' are considered as 'super-stages' in this chart.

Marine stage / zone divisions

Isotope studies from the bottom sediments of the world's oceans have indicated that as many as 52 cold and interposed warm climate periods, often referred to as glacials and interglacials, occurred during the last 2.6 million years. In contrast to the deep sea, continental evidence is so incomplete and regionally variable that terrestrial glacial-interglacial stratigraphies must refer to the ocean record for a global chronological foundation.

Here the deep-sea based, climatically-defined chronostratigraphy is taken from oxygen isotope data collected and processed by A.J. Crowhurst (Delphi Project, 2002). It is plotted against the magnetostratigraphic time scale prepared and modified from Funnell (1996). The curve plots depict $\delta^{18}O$ (the ratio of ^{18}O versus ^{16}O) in the tests of fossil benthonic (ocean-floor dwelling) foraminifera. Shifts in this ratio are a measure of global ice-volume, which is dependent on global temperature and which determines global sea-level. Planktonic foraminifera and calcareous nannoplankton provide an alternative biostratigraphical means of subdivision of marine sediments. The microplaeontological zonation is taken from Berggren *et al.* (1995).

Antarctic ice-core records

Two plots of isotope measurements from Antarctic ice-cores are shown. The first is the 420 km-long plot from the Vostok core and shows atmospheric $\delta^{18}O$ (Petit *et al.*, 1999), determined from gas bubbles in the ice. This atmospheric $\delta^{18}O$ is inversely related to $\delta^{18}O$ measurements from seawater and therefore is a measure of ice-volume. It can also be used to separate ice volume and deep-water temperature effects in benthic foraminiferal $\delta^{18}O$ measurements. The deuterium measurements (δD) for the last 740 kyr are from the 3.2 km deep EDC core in Dome C (EPICA community members, 2004). They come from samples of the ice itself and give a direct indication of Antarctic surface palaeotemperature.

Regional stage/substage divisions

The continuous sequences provide the comparisons for a selection of continental and shallow marine stage-successes from around the world reconstructed from discontinuous sediment successions. Solid horizontal lines on the plots indicate observed boundaries, where no lines separate stages, additional events may potentially be recognised in the future.
The plot from the Chinese loess deposits shows the sequence of palaeosols (indicated by S and W/S) and alternating loess units (L and WL) from Liuchiawo (Xu Zhidong *et al.*, 1990). It is accompanied by a continuous plot of magnetic susceptibility from the same sequence.

The NW European stages are taken from Zagwijn (1992) and De Jong (1988). The British stages are taken from Mitchell *et al.* (1973), Gibbard *et al.* (1991) and Bowen (1999). The Russian Plain stages are from the Stratigraphy of the USSR, Quaternary System (1982, 1984), Krasnenkov Ioasifova & Semakov (1997), Shik, Borisov & Zarrina (2002), Ioasifova *et al.* (2002, modified 2004) and Troitsky (unpublished). In addition, the Russian Pleistocene is also frequently divided into the Eopleistocene, equivalent to the Early Pleistocene Subseries, and the Neopleistocene, equivalent to the Middle and Late Pleistocene subseries. The North American stages are taken from Richmond (unpublished). The New Zealand stages are from Pillans (1991) and Ikin (2004).

Anthropocene

A recent proposal has been made to establish a new series status division following the Holocene, to be termed the Anthropocene. The term is being increasingly employed to identify the current issue of anthropogenic global environmental change, and may be adopted on stratigraphical grounds. It might be adopted at formal Series/Epoch level, for the time since the start of the Industrial Revolution when changes sufficient to leave a global stratigraphic signature distinct from that of the Holocene or of pervious Pleistocene interglacial phases, occurred. A boundary definition may be made either using a Global Stratigraphic Section and Point ('golden spike') localities, and or by adopting a numerical date (GSSA). Formal adoption of this term depends on its utility, particularly to Earth Scientists working on late Holocene successions (Zalasiewicz *et al.* 2008). Because of its' short time duration, it has not been included in the chart.

References

Full bibliographic references are found on the web site: http://www.quaternary.stratigraphy.org.uk/

Acknowledgements

The compilers are grateful to the many people and sponsors who have assisted in the production of this chart. In particular, they thank: Alan Ion, Vincent Crowhurst, Victoria Hall, Martin Head, Wan Hesk, Thijs van Kolfschoten, Thomas Litt, Leszek Marks, Jason Ogg, Brad Pillans, Chris Reilly, Nick Shackleton (†), Aleksey Sorokin, Charles Turner, Mike Walker, Wim Westerhoff and Eric Wolff.

Общая стратиграфическая шкала четвертичной системы

Общие стратиграфические подразделения					Основные хронологические рубежи (млн лет)	Геохронологические подразделения				
Система	Надраздел (отдел)	Раздел (подотдел)	Звено	Ступень		Период	Эпоха	Фаза	Пора	Термохрон, криохрон
Четвертичная (квартер) Q	Голоцен Q_h						Голоценовая			
	Плейстоцен Q_p	Неоплейстоцен Q_N^o	Верхнее	Четвертая	- 0,01 -	Четвертичный (квартер)	Плейстоценовая	Неоплейстоценовая	Поздняя	Поздний криохрон
				Третья						Поздний термохрон
				Вторая						Ранний криохрон
				Первая						Ранний термохрон
			Среднее						Средняя	
			Нижнее						Ранняя	
		Эоплейстоцен Q_E	Верхнее		0,8 -			Эоплейстоценовая	Поздняя	
			Нижнее						Ранняя	
Неогеновая	Плиоцен	Верхний			- 1,8 -	Неогеновый	Плиоценовая			

Примечание. Шкала утверждена МСК 1995 г. и опубликована в Дополнениях к Стратиграфическому кодексу России (2000).

Рис. 1. Стратиграфическая схема четвертичных отложений Центра Восточно-Европейской платформы. В графе «Палеомагнетизм» показаны только эпизоды (субзоны), надежно установленные в этом регионе (а — лог Красный, б — Харамилло, в — Олдувей). Значение индексов объяснено в тексте:

1 — почвы (e_p), 2 — лессовиды (L); 3 — границы аллювиальных свит

Шик, 2004

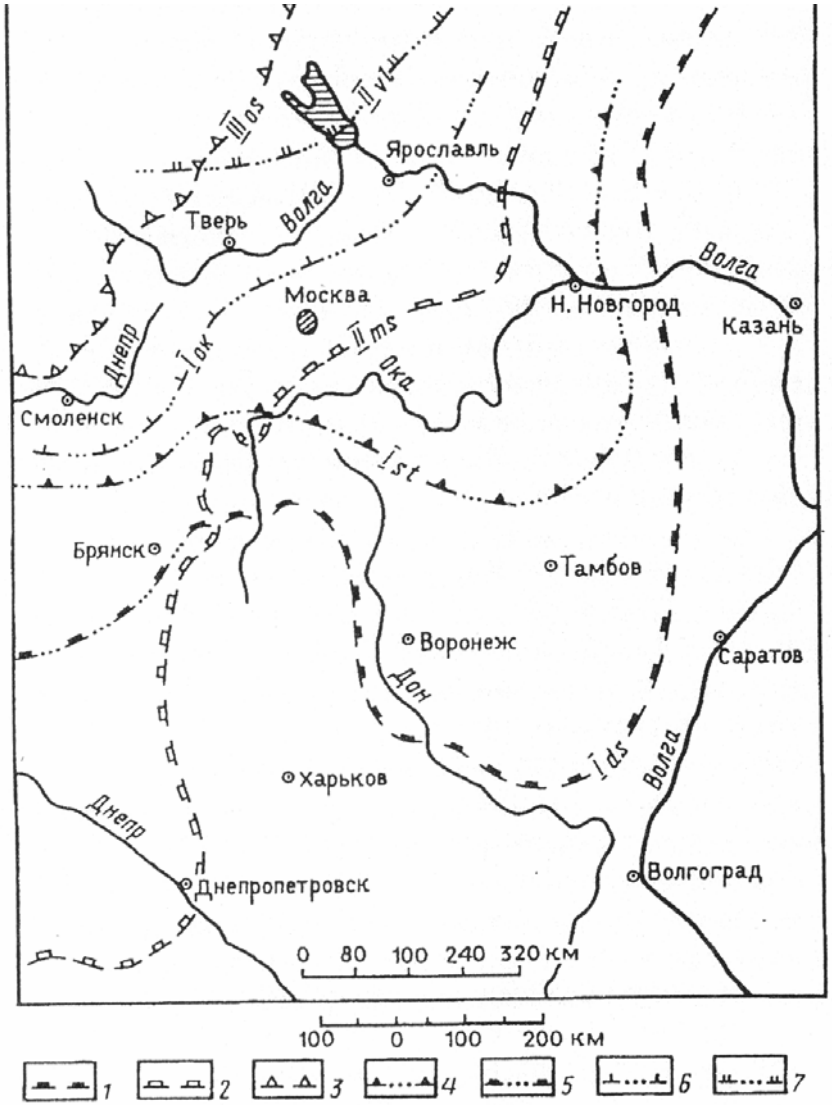

Рис. 2. Распространение оледенений в Центре Восточно-Европейской платформы:

1–3 — границы оледенений: 1 — донского, 2 — московского, 3 — осташковского; 4–7 — погребенные границы оледенений: 4 — сетуньского, 5 — донского, 6 — окского, 7 — вологодского

Шик, 2004


Ice sheet extent at 90 ka
Svalbard
Barents Sea
Kara Sea
Lake Komi
Urals
Quaternary glaciation limit
Caspian Sea
Aral Sea

ОЛЕДЕНЕНИЯ ЧЕТВЕРТИЧНОГО ПЕРИОДА

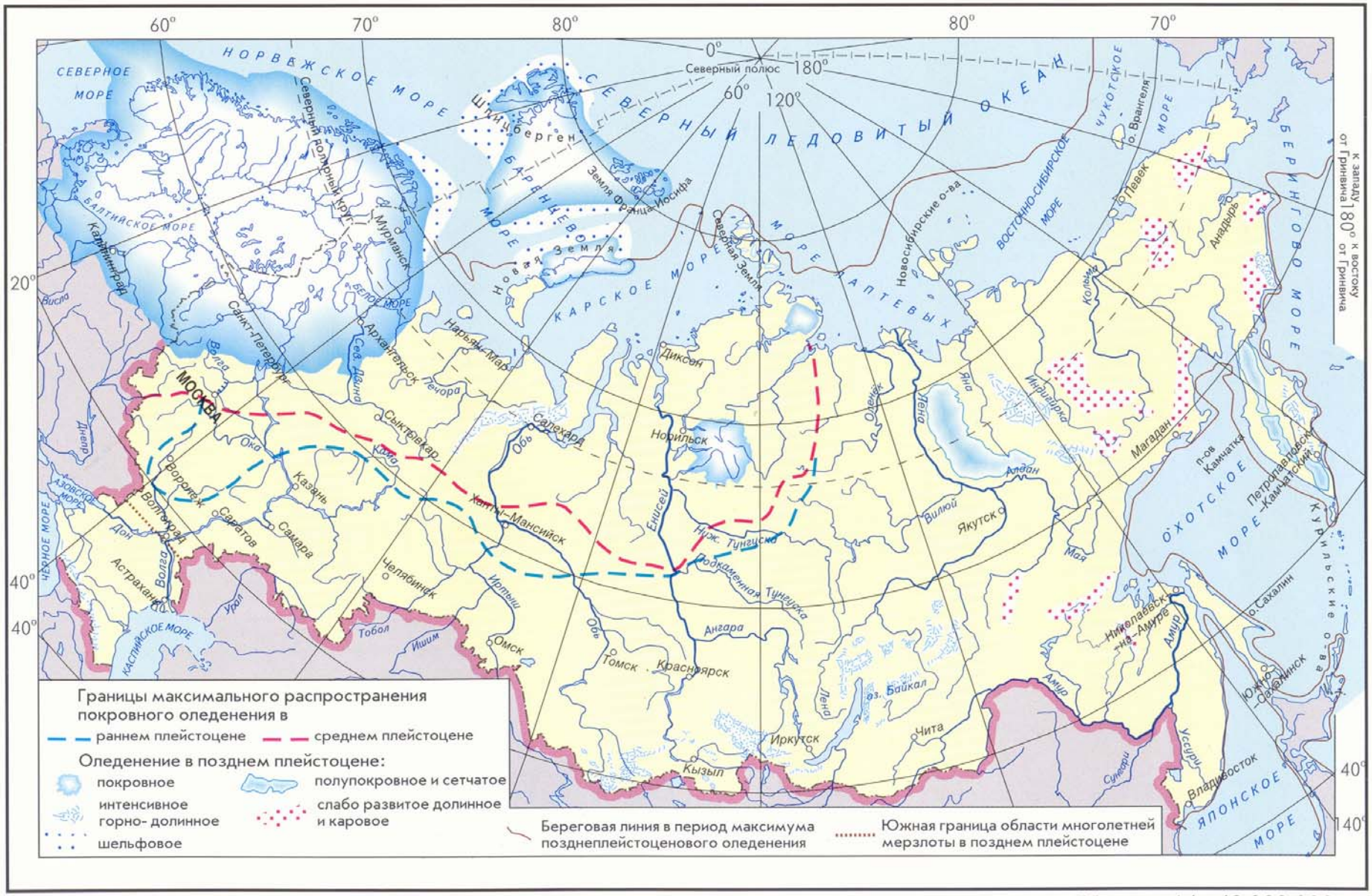

Масштаб 1 : 40 000 000

Современные ледники

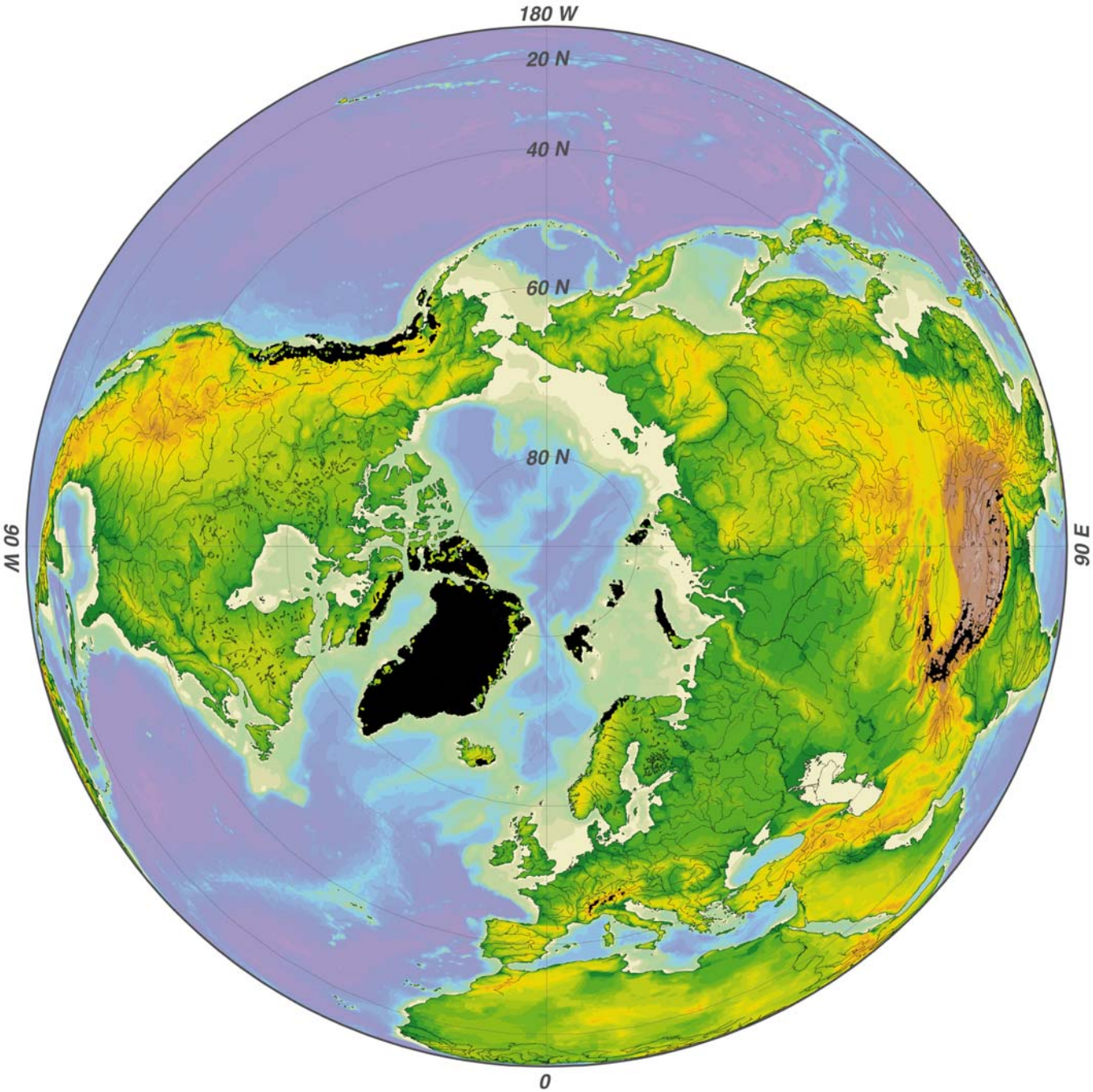

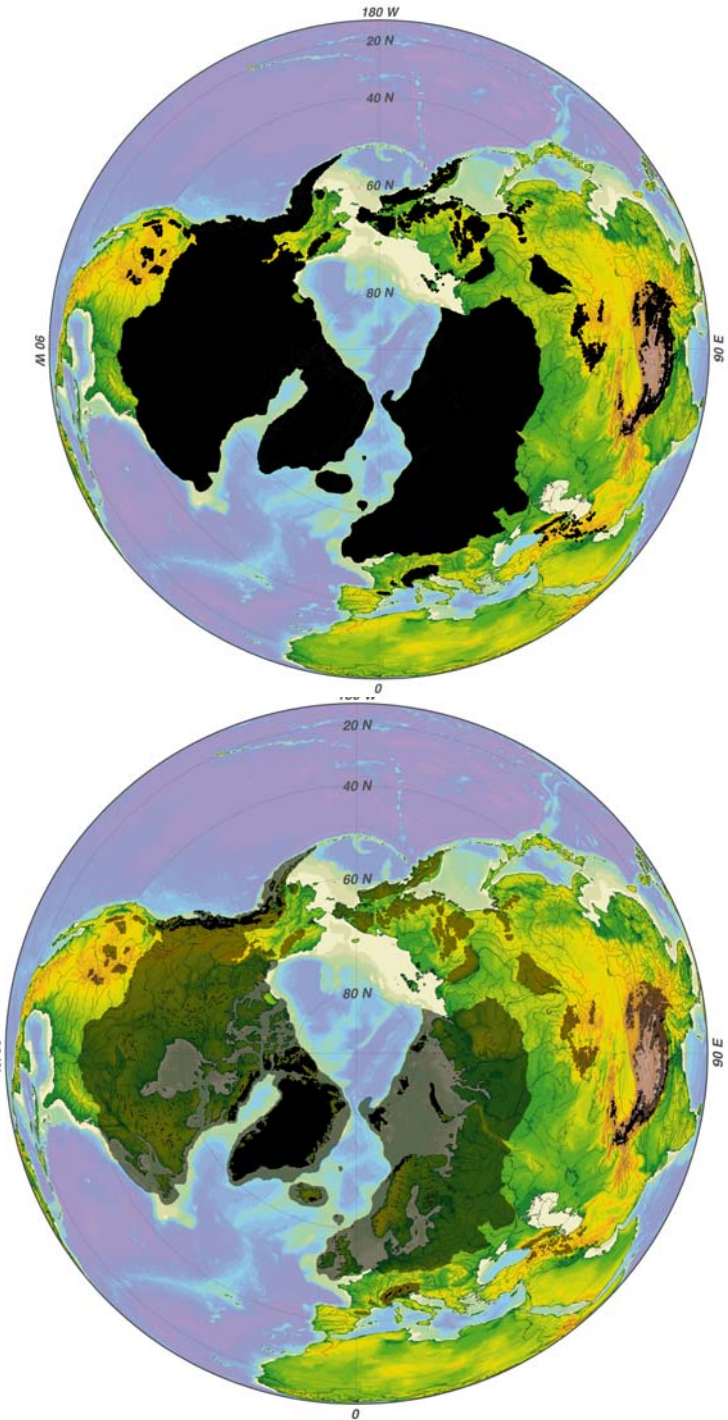

Контуры области максимального ледника

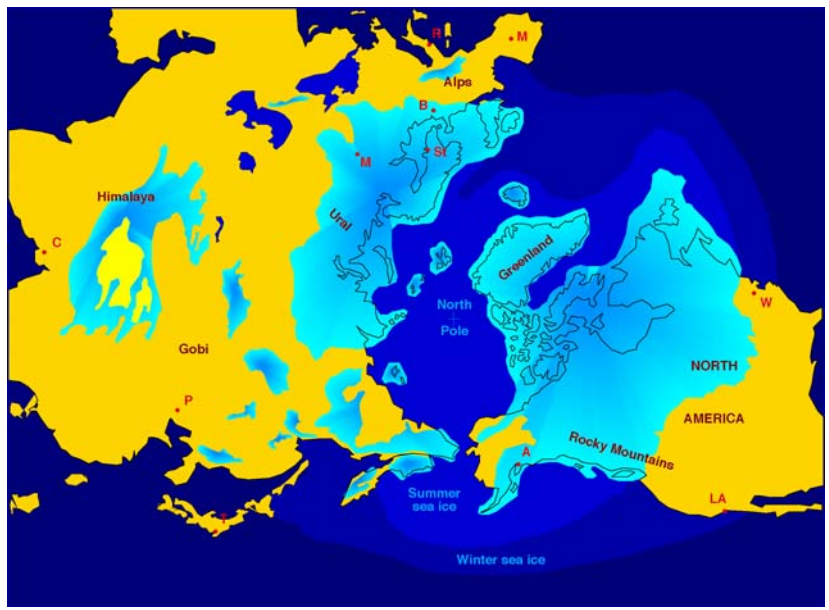

LAST GLACIAL MAXIMUM

20-18 Ka

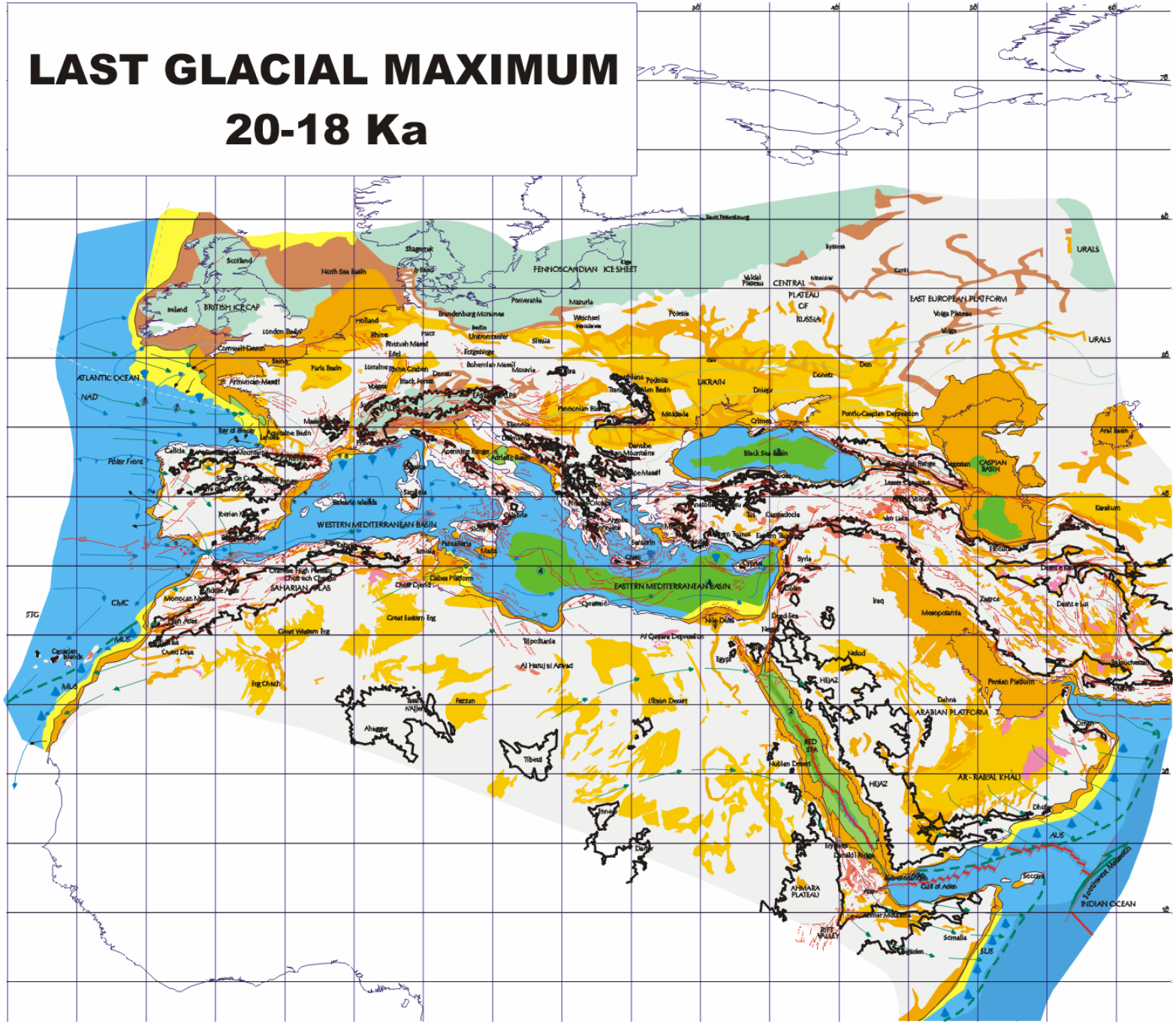
FENNOSCANDIAN ICE SHEET
BRITISH ICE CAP
ATLANTIC OCEAN
NAD
CENTRAL PLATEAU OF RUSSIA
EAST EUROPEAN PLATFORM
URALS
CASPIAN BASIN
Black Sea Basin
Pontic-Caspian Depression
UKRAIN
Podolia
Moldavia
Crimea
Don
Donetz
Dniepr
Volga Plateau
Pannonian Basin
Danube Delta
Danubian Mountains
Rhodope Massif
Apennine Range
Adriatic Basin
Tyrrhenian Basin
Sardinia
Corsica
Balearic Islands
WESTERN MEDITERRANEAN BASIN
EASTERN MEDITERRANEAN BASIN
Ionian Basin
Cyrenaic
Nile Delta
Egypt
Libya
Tripolitania
Al Hamuj al Aswad
Fezzan
Ghadames
Ghadames Basin
Hamada el Hamra
Tibesti
Ahaggar
Tassili n'Ajjer
Ilgh Chech
Great Eastern Erg
Great Western Erg
Chott ech Chergui
Chott Djerid
Gabes Platform
SAHARIAN ATLAS
Moroccan Meseta
High Atlas
Anti Atlas
Oued Draa
Canarian Islands
CMC
MOR
MLS
STG
Poter Front
Celtic Sea
Bay of Biscay
Aquitaine Basin
Paris Basin
Armorican Massif
Ireland
Scotland
North Sea Basin
Skagerrak
Jylland
Rhine
Rhenish Massif
Eifel
Lorraine
Rhine Graben
Black Forest
Vosges
Bohemian Massif
Moravia
Silesia
Brandenburg Moraines
Pomerania
Masuria
Polesia
Weichsel
Warszawa
Berlin
Holland
London Basin
Cornwall-Devon
Wales
Saint Petersburg
Valdai Plateau
Moscow
Kazan
Syria
Iraq
Mesopotamia
Zagros
Dasht e Lut
Dasht e Kavir
Karakum
Aral Basin
Lesser Caucasus
Caucasus
Dagestan
Kura
Van Lake
Cappadocia
Taurus
Eastern Taurus
Iskenderun
Adana
Cyprus
Rhodes
Crete
Malta
Pantelleria
Sicily
Tyrrhenian Sea
Ionian Sea
Aegean Sea
Marmara
Bosporus
Dardanelles
Thrace
Macedonia
Thessaly
Peloponnesus
Athens
Corinth
Gulf of Corinth
Gulf of Patras
Epirus
Albania
Dinarides
Slovenia
Istria
Venice
Po Valley
Milan
Turin
Alps
Switzerland
Jura
Rhone
Massif Central
Auvergne
Cevennes
Languedoc
Provence
Rhone Delta
Camargue
Pyrenees
Ebro Basin
Catalonia
Valencia
Balearic Islands
Iberian Massif
Iberian Range
Meseta
Duero Basin
Tagus Basin
Guadiana Basin
Guadalquivir Basin
Betic Cordillera
Alboran Sea
Gibraltar
Strait of Gibraltar
Canary Islands
Madeira
Azores
Mid-Atlantic Ridge
Bay of Biscay
Celtic Sea
Irish Sea
Wales
Cornwall-Devon
Ireland
Scotland
Norwegian Sea
Iceland
Greenland
Baffin Bay
Labrador Sea
Hudson Bay
Newfoundland
Gulf of St. Lawrence
Nova Scotia
Prince Edward Island
New Brunswick
Maine
Boston
New York
Philadelphia
Washington
Virginia
North Carolina
South Carolina
Georgia
Florida
Florida Keys
Gulf of Mexico
Mississippi
Louisiana
New Orleans
Texas
Houston
Galveston
Corpus Christi
Rio Grande
Mexico
Monterrey
Sierra Madre Oriental
Sierra Madre Occidental
Baja California
Gulf of California
Pacific Ocean
Hawaii
Alaska
Aleutian Islands
Bering Sea
Bering Strait
Chukchi Sea
Beaufort Sea
Arctic Ocean
Canada
Yukon
Northwest Territories
Nunavut
Hudson Strait
Ungava Bay
Quebec
Ontario
Manitoba
Saskatchewan
Alberta
British Columbia
Great Lakes
Lake Superior
Lake Michigan
Lake Huron
Lake Erie
Lake Ontario
Chicago
Detroit
Toronto
Ottawa
Montreal
Quebec City
Minneapolis
Saint Paul
Duluth
Fargo
Grand Forks
Bismarck
Dakotas
Nebraska
Kansas
Oklahoma
Missouri
Arkansas
Tennessee
Kentucky
West Virginia
Pennsylvania
New York
Vermont
New Hampshire
Maine
Rocky Mountains
Colorado
Denver
Utah
Nevada
Las Vegas
Arizona
Phoenix
Tucson
New Mexico
Albuquerque
Wyoming
Montana
Idaho
Boise
Oregon
Portland
Seattle
Washington
San Francisco
Los Angeles
San Diego
California
Central Valley
Sierra Nevada
Cascade Range
Mount Rainier
Mount Shasta
Yellowstone
Grand Canyon
Colorado River
Rio Grande
Mississippi River
Missouri River
Ohio River
Tennessee River
Cumberland River
Arkansas River
Red River
Columbia River
Snake River
Hudson River
Saint Lawrence River
Great Salt Lake
Salton Sea
Death Valley
Mojave Desert
Sonoran Desert
Chihuahuan Desert
Great Basin
Colorado Plateau
Appalachian Mountains
Blue Ridge Mountains
Shenandoah Valley
Chesapeake Bay
Delaware Bay
Cape Cod
Martha's Vineyard
Nantucket
Long Island
Manhattan
Brooklyn
Queens
Bronx
Staten Island
Jersey City
Newark
Trenton
Atlantic City
Wilmington
Baltimore
Annapolis
Richmond
Norfolk
Virginia Beach
Raleigh
Charlotte
Greensboro
Asheville
Great Smoky Mountains
Knoxville
Nashville
Memphis
Atlanta
Savannah
Charleston
Jacksonville
Tallahassee
Orlando
Tampa
Miami
Key West
Everglades
Okefenokee Swamp
Birmingham
Montgomery
Mobile
Gulf Coast
Pensacola
Biloxi
Gulfport
Baton Rouge
New Orleans
Lafayette
Lake Pontchartrain
Lake Maurepas
Lake Borgne
Mississippi Delta
Shreveport
Dallas
Fort Worth
Austin
San Antonio
Houston
Galveston
Corpus Christi
Padre Island
Rio Grande Valley
Brownsville
Laredo
Del Rio
Big Bend
Guadalupe Mountains
Carlsbad Caverns
Roswell
Albuquerque
Santa Fe
Taos
Rio Grande Gorge
Sangre de Cristo Mountains
Pecos River
Llano Estacado
Amarillo
Lubbock
Abilene
Wichita Falls
Oklahoma City
Tulsa
Wichita
Kansas City
Topeka
Lincoln
Omaha
Sioux City
Des Moines
Cedar Rapids
Iowa City
Davenport
Quad Cities
Rock Island
Peoria
Springfield
Champaign
Urbana
Chicago
Gary
Indianapolis
Fort Wayne
South Bend
Evansville
Louisville
Lexington
Cincinnati
Columbus
Dayton
Toledo
Cleveland
Akron
Youngstown
Pittsburgh
Erie
Buffalo
Rochester
Syracuse
Albany
Utica
Binghamton
Scranton
Wilkes-Barre
Allentown
Bethlehem
Easton
Reading
Lancaster
Harrisburg
York
Gettysburg
Hagerstown
Frederick
Baltimore
Washington
Annapolis
Dover
Wilmington
Philadelphia
Trenton
Princeton
New Brunswick
Newark
Jersey City
Hoboken
Staten Island
Brooklyn
Queens
Bronx
Manhattan
Long Island
Nassau
Suffolk
Montauk
Hamptons
Fire Island
Jones Beach
Coney Island
Rockaway
Jamaica Bay
Kennedy Airport
LaGuardia Airport
Newark Airport
Teterboro Airport
Meadowlands
Secaucus
Hackensack
Paterson
Passaic
Clifton
Wayne
Morristown
Parsippany
Dover
Rockaway
Boonton
Montclair
Glen Ridge
Bloomfield
Nutley
Belleville
Kearny
Harrison
East Orange
Orange
South Orange
Maplewood
Irvington
Union
Elizabeth
Linden
Roselle
Roselle Park
Cranford
Garwood
Westfield
Scotch Plains
Fanwood
Plainfield
North Plainfield
Dunellen
Bound Brook
Somerville
Manville
Raritan
Hillsborough
Millstone
Princeton
Lawrenceville
Hopewell
Pennington
Ewing
Lawrence
West Windsor
East Windsor
Hightstown
Cranbury
South Brunswick
Monroe
Jamesburg
Helmetta
Spotswood
Old Bridge
Sayreville
South Amboy
Perth Amboy
Woodbridge
Carteret
Rahway
Clark
Linden
Roselle
Roselle Park
Union
Elizabeth
Hillside
Irvington
Maplewood
South Orange
Orange
East Orange
Harrison
Kearny
Secaucus
Hoboken
Jersey City
Bayonne

PALEOMAP – Early Oligocene

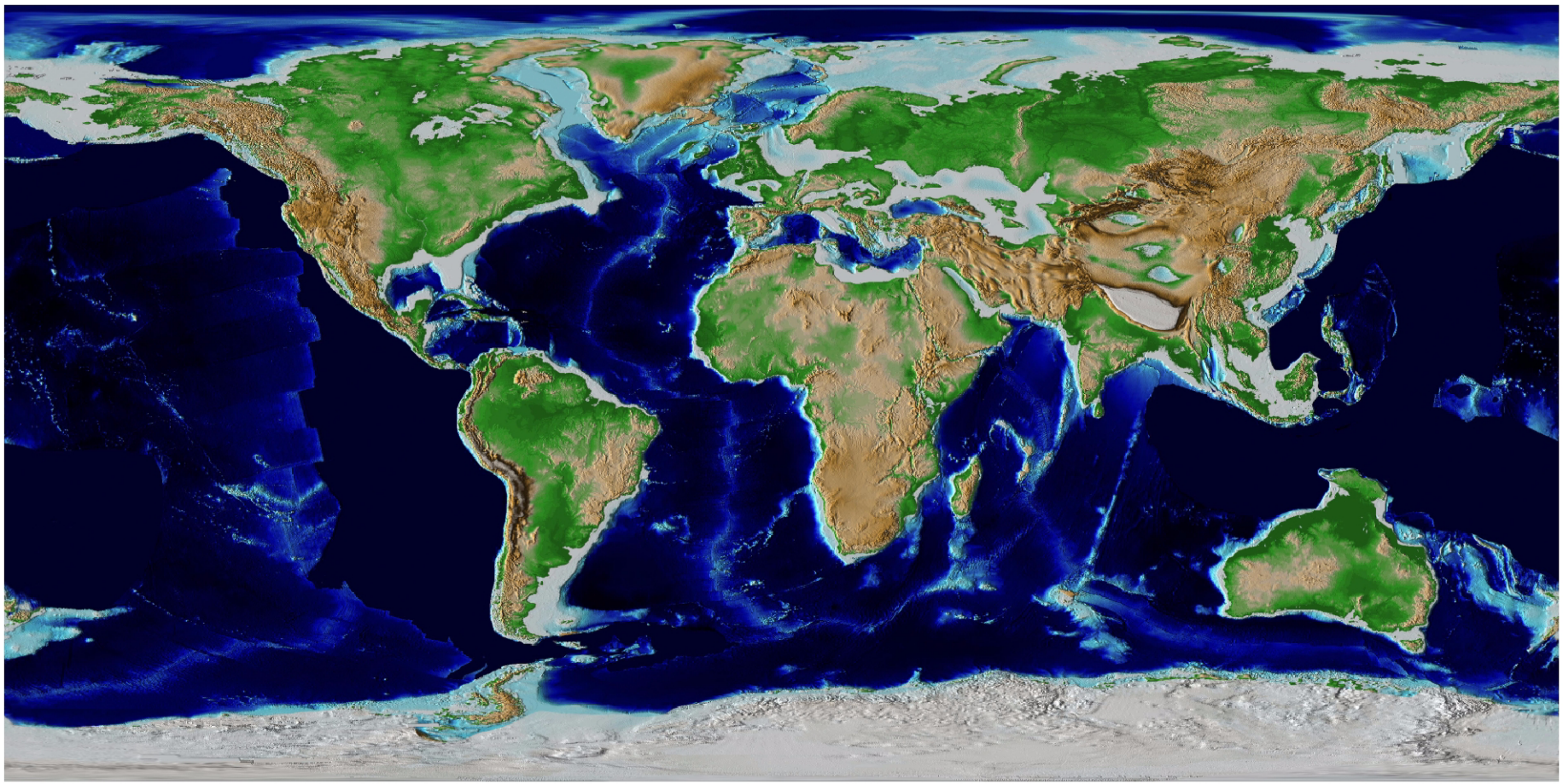

PALEOMAP – Mid Miocene

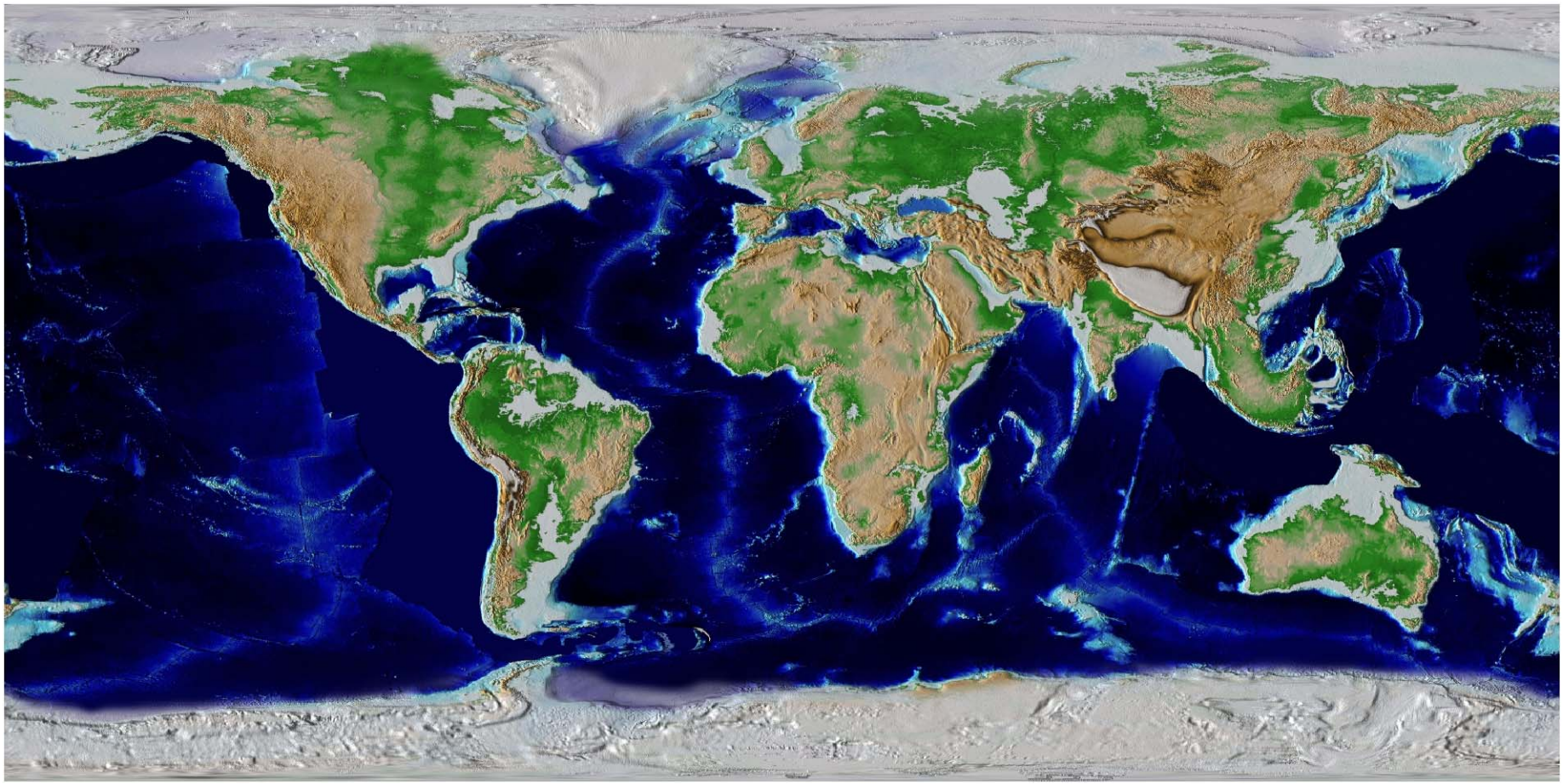

PALEOMAP – Mid/Late Miocene

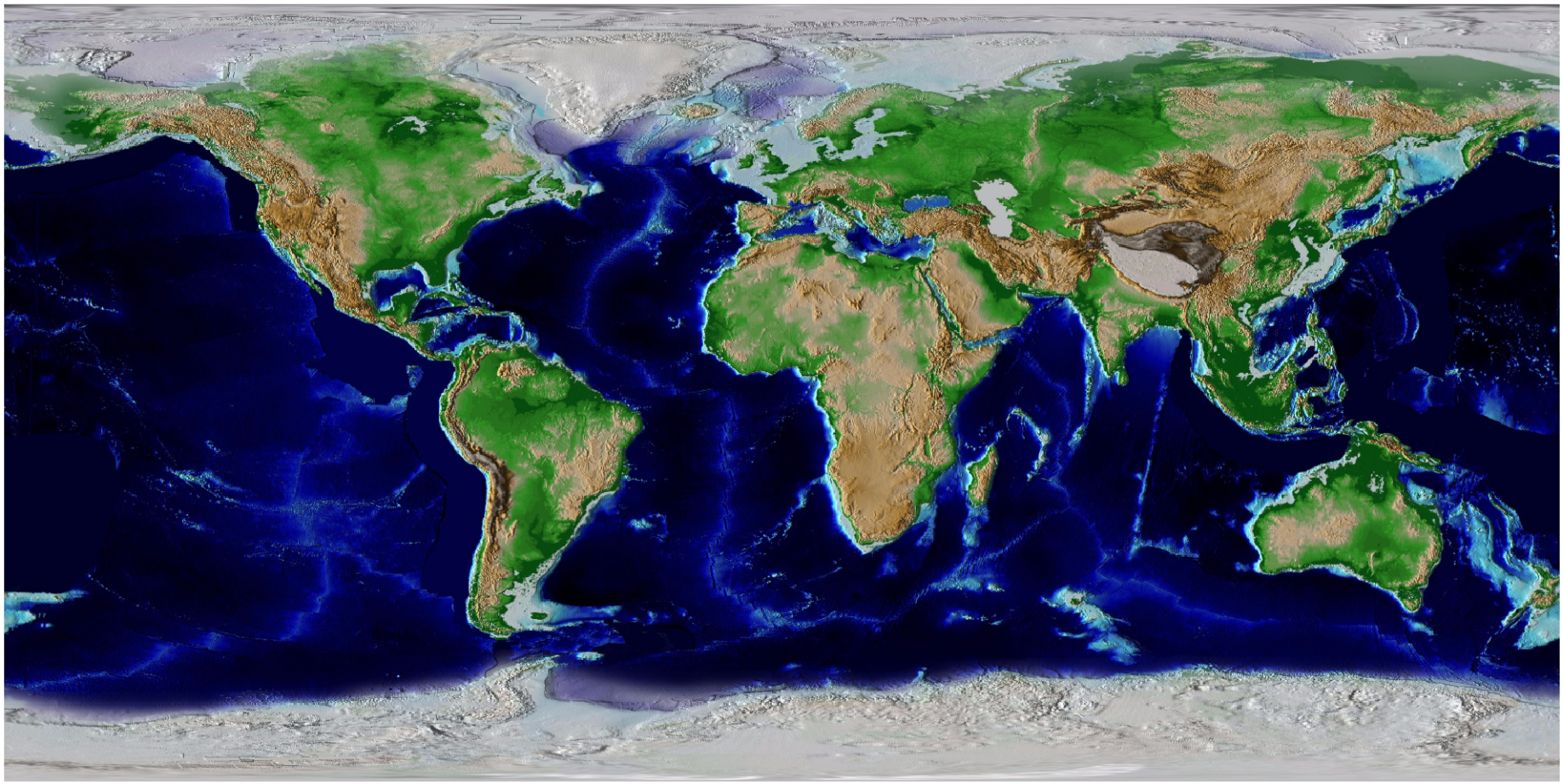

PALEOMAP – Present Day